

1
2
3
4 **Hf and Nd isotopes in Early Ordovician to Early Carboniferous granites as**
5
6 **monitors of crustal growth in the Proto-Andean margin of Gondwana**
7
8
9

10 **Juan A. Dahlquist^{1,2}, Robert J. Pankhurst³, Richard M. Gaschnig⁴, Carlos W. Rapela⁵, César Casquet⁶,**
11 **Pablo H. Alasino^{7,2}, Carmen Galindo⁶, Edgardo G. Baldo¹**

12 ¹ICTERRA-CONICET-UNC, Av. Vélez Sarsfield 1611, Pab. Geol., X5016CGA, Córdoba, Argentina

13 ²INGeReN-CENIIT-UNLaR, Av. Gob. Vernet y Apóstol Felipe. 5300, La Rioja, Argentina

14 ³British Geological Survey, Keyworth, Nottingham NG12 5GG, UK

15 ⁴Department of Geology University of Maryland College Park, Maryland 20742, USA

16 ⁵CIG-CONICET-UNLP, Calle 1 N° 644, 1900, La Plata, Argentina

17 ⁶Universidad Complutense 28040 Madrid, Spain

18 ⁷CRILAR-CONICET, Entre Ríos y Mendoza. 5301, Anillaco, La Rioja, Argentina

24
25 **ABSTRACT**
26

27 We report the first study integrating *in situ* U–Pb and Hf isotope data from magmatic zircon and
28
29 whole-rock Sm–Nd isotope data for granitic rocks of the Sierras Pampeanas, Argentina, in order to
30
31 evaluate the Palaeozoic growth of the proto-Andean margin of Gondwana. Generation of Ordovician
32
33 magmas dominantly involved crustal reworking and stabilization rather than the formation of new
34
35 continental crust by juvenile material accretion, whereas Late Palaeozoic magmatism produced some
36
37 limited continental growth, especially during the Early Carboniferous. Overall, the proto-Andean
38
39 margin was shaped predominantly by the reworking of existing old crustal rocks rather than crustal
40
41 growth.
42
43

44 **Keywords:** U-Pb dating, Hf and Nd isotopes, zircon, crustal growth.

45
46
47

48 23
49
50

51
52 25
53

54 26
55

56
57 27
58

59 28
60

61
62

63
64

65

1
2
3 29 **1. Introduction**
4
5

6 30 As the pre-eminent U–Pb geochronometer zircon plays a key role in crustal evolution studies.
7

8 31 Recent analytical advances permit investigation of complex zircon grains at high spatial resolution,
9
10 32 where the goal is to link U–Pb ages to other geochemical information, such as Hf isotopic
11
12 33 composition. Thus zircon can provide time-stamped ‘snapshots’ of Hf isotope signatures of magmas
13
14 34 throughout Earth’s history, even at the scale of individual growth zones within a single grain. This
15
16 35 information is an invaluable help to geochemists trying to distinguish magmatic events that added
17
18 36 new mantle-derived material to the continental crust from those that recycled existing crust (e.g.,
19
20 37 [Scherer et al., 2007](#); [Siebel and Chen, 2010](#)).
21
22
23
24

25 38 In this article we report in situ U–Pb and Hf isotope data from zircons and whole-rock Sm/Nd data
26
27 39 from their host granites to evaluate the origin of the granitic magmas and consequently the building
28
29 40 of the proto-Andean margin of Gondwana during three main Palaeozoic magmatic events known in
30
31 41 the Sierras Pampeanas of NW Argentina.
32
33
34
35 42
36
37
38 43 **2. Regional setting**
39

40 44 The proto-Andean margin of Gondwana is a good example of an accretionary orogen that has
41
42 45 been active since at least the Early Ordovician up to the present ([Cawood, 2005](#)), leading to the
43
44 46 formation of different plutonic rocks during the Palaeozoic. Geochronological data and their
45
46
47 47 interpretation in terms of major magmatic episodes allow the recognition of four main granitoid
48
49 48 groups in the Eastern Sierras Pampeanas of NW Argentina ([Fig. 1](#)): Early Cambrian (Pampean),
50
51 49 Early–Middle Ordovician (Famatinian), Middle-Late Devonian (Achalian) and Early Carboniferous.
52
53 50 We have studied granitic rocks from the last three of these groups. Famatinian granitoids are typical
54
55 51 calc-alkaline granites, formed in an active continental margin; those emplaced during the Achalian
56
57 52 and Early Carboniferous events have dominantly A-type signatures.
58
59
60
61
62
63
64
65

1
2
3 53 The Famatinian arc (Fig. 1) is widely accepted to have been constructed on continental crust
4
5
6 54 (Pankhurst et al., 1998; Dahlquist and Galindo, 2004; Miller and Söllner, 2005; Dahlquist et al.,
7
8 55 2008). In the Famatinian magmatic belt of the Sierras Pampeanas, Pankhurst et al. (2000) identified
9
10 56 three distinct granite-types: dominant I-type, small-scale S-type, and tonalite-trondhjemite-
11
12 57 granodiorite (TTG, confined to the Sierras de Córdoba, see Fig. 1 of Pankhurst et al., 2000). These
13
14 58 three granite types can be distinguished petrologically, geochemically, and spatially, although all
15
16 59 were emplaced within the 484–463 Ma interval (see also Dahlquist et al., 2008). Detailed
17
18 60 petrological and geochemical studies of these rocks are given by Aceñolaza et al. (1996), Saavedra et
19
20 61 al. (1998), Pankhurst et al. (1998, 2000), Dahlquist and Galindo (2004), Miller and Söllner (2005),
21
22 62 Dahlquist (2002), Dahlquist et al. (2005, 2007, 2008), and Ducea et al. (2010).

23
24 63 The widespread Famatinian magmatism yielded extensive I-type intrusions (mostly tonalite,
25
26 64 granodiorite and minor monzogranite and gabbro) with $\epsilon_{\text{Nd}_t} = -3$ to -6 (data from Pankhurst et al.
27
28 65 1998, 2000; Dahlquist and Galindo 2004; Dahlquist et al., 2008). Some gabbros in the Sierra de
29
30 66 Valle Fértil reached a more radiogenic value of $\epsilon_{\text{Nd}_t} = -2.4$, and subordinate small-scale isolated
31
32 67 Ordovician plutons of Na-rich granite located in the Pampean belt foreland (TTG suites) have $\epsilon_{\text{Nd}_t} =$
33
34 68 +1.6 to -0.2 . Most of the granitic rocks have T_{DM} model ages between 1.7 and 1.5 Ga and Nd
35
36 69 isotopic signatures suggesting derivation from a composite Palaeo-Mesoproterozoic lithospheric
37
38 70 section that included lower and upper crustal sources as well as the sub-lithospheric mantle (Rapela
39
40 71 et al. 2008a; Dahlquist et al. 2008 and references therein). Thus, with the exception of the minor
41
42 72 TTG suites, it is usually argued that the Famatinian magmatic arc reworked old lithospheric sources,
43
44 73 with very little addition of juvenile material, although this view may need a degree of modification
45
46 74 since the discovery of more juvenile Nd isotope compositions in the extreme west of the Sierra de
47
48 75 Valle Fértil (Casquet et al., submitted).

1
2
3 Dahlquist et al. (2008) concluded that: (i) the Famatinian magmatism was brief (~ 484 to ~ 463
4 Ma), in remarkable contrast to the long-lived Mesozoic-Cenozoic cordilleran magmatism of the
5 Andes; and (ii) the Early to mid-Ordovician development of ensialic marine basins was synchronous
6 with the emplacement of voluminous lithosphere-derived magmatism in the central region of the
7 Famatinian orogenic belt, which strongly contrasts with the Andean-type model for the production of
8 magmas (Dahlquist and Galindo, 2004; Rapela et al., 2008a). This magmatism was completely
9 extinguished during the mid-Ordovician and the marine sedimentary basins closed in the early Late
10
11 Ordovician.

12
13 The ca. 2500 m² Achala batholith in the Sierras de Córdoba (Fig. 1) was emplaced during the
14 Middle–Late Devonian 368±25 Ma U–Pb zircon, Dorais et al. (1997); 393±5 Ma U–Pb SHRIMP
15 zircon, Stuart-Smith et al. (1999); 382±5 Ma Siegesmund et al. (2004); 369±9 Ma Rb–Sr whole-
16 rock, Pinotti et al. (2006) and 379±4 and 369±3 Ma U–Pb SHRIMP zircon, Rapela et al. (2008b)
17 (Fig. 1). It is the largest of a series of intrusive granitic bodies in the Sierras Pampeanas that are
18 conspicuously discordant to structures and rocks formed during the Cambrian (Pampean) and
19 Ordovician (Famatinian) metamorphic events. Contact aureoles indicate shallow emplacement,
20 usually less than 2 kbar (e.g., Baldo, 1992; Pinotti et al., 2002). Rapela et al. (2008b) concluded that
21 the Achala batholith has an A-type signature. Sims et al. (1998), Stuart-Smith et al. (1999), and
22 Siegesmund et al. (2004) considered the voluminous Devonian intrusive rocks in the Sierras de
23 Córdoba and the eastern area of the Sierras de San Luis to have been emplaced during compression
24 associated with Late Devonian low-grade shear zones, together defining the Achalian orogeny.
25 According to this interpretation the Devonian granites, such as the Achala (Sims et al., 1998) and
26 Cerro Áspero batholiths in Sierra de Córdoba (e.g., Pinotti et al., 2002, 2006), and the Las Chacras
27 (Siegesmund et al., 2004) and Renca (Stuart-Smith et al., 1999) batholiths in Sierra de San Luis (Fig.
28 1), are not post-orogenic intrusions of the Famatinian Orogeny as proposed by Pankhurst and Rapela
29
30
31
32
33
34
35
36
37
38
39
40
41
42
43
44
45
46
47
48
49
50
51
52
53
54
55
56
57
58
59
60
61
62
63
64
65

(1998), but belong to a distinct tectonomagmatic event. The Late Devonian compressional event is controversial and has been related to: i) collision of the suggested Chilenia terrane with the proto-Pacific margin (Willner et al., 2011), ii) final collision between the Famatinian magmatic arc and the Pampean hinterland (Höckenreiner et al., 2003) and, recently, iii) push–pull tectonic switching episodes during Devonian and Carboniferous time, resulting from flat-slab/roll-back subduction in the Pacific margin (Alasino et al., 2012). The A-type geochemical signature of the Achala batholith (Rapela et al., 2008b) strongly suggests generation of intacratonic magmas in a dominantly extensional regime with subsequent lithosphere thinning (Early-Middle Devonian?), followed by Late Devonian horizontal shortening and Early Carboniferous lithosphere stretching (see tectonic switching model of Collins, 2002).

In Carboniferous times, isolated and scattered granitic pluton with anorogenic signature occurred along more than 1000 km in the Sierras Pampeanas of NW Argentina (see Dahlquist et al., 2010, Fig. 1). It is represented by small and scattered plutons, usually sub-circular, intruded mainly along prominent shear zones active in the Early Carboniferous (Dahlquist et al., 2010). Host rocks to this Carboniferous magmatism formed during three main periods of magmatic and metamorphic activity: Middle Cambrian (Pampean orogeny), Early–Middle Ordovician (Famatinian orogeny), and Middle–Late Devonian (Achalian event) (Pankhurst et al., 1998, 2000; Rapela et al., 1998; Sims et al., 1998; Dahlquist et al., 2008; Rapela et al., 2008b; Vaughan and Pankhurst, 2008; Spagnuolo et al., 2011; Tohver et al., 2011; Alasino et al., 2012).

The geodynamic setting of the Carboniferous magmatism remains controversial. Some authors have suggested that it resulted from crustal reheating as the final phase of a protracted Famatinian orogeny extending from Ordovician to Early Carboniferous (e.g., Grissom et al., 1998; Llambías et al., 1998; Höckenreiner et al., 2003; Grosse et al., 2009). Others have argued for a distinctive and extended Achalian orogenic event in the Devonian–Early Carboniferous (e.g., Sims et al., 1998;

1
2
3 124 [Stuart-Smith et al., 1999](#); [Siegesmund et al., 2004](#); [López de Luchi et al., 2004](#); [Dahlquist et al.,](#)
4
5 125 [2006](#); [Rapela et al., 2008b](#)). Recently, [Dahlquist et al. \(2010\)](#) claimed that the Early Carboniferous
6
7 126 A-type granites of the Eastern Sierras Pampeanas represent a tectonothermal event distinct from both
8
9 127 Famatinian and Achalian magmatism. Field and geochemical data for the Early Carboniferous
10
11 128 granites of the Eastern Sierras Pampeanas are indicative of a distinctive extensional within-plate
12
13 129 magma setting where compressive tectonic regime is absent ([Dahlquist et al., 2010](#)).
14
15
16
17

18 130 In summary, Devonian and Carboniferous magmatism would have been developed in an
19
20 131 intracratonic orogen related to continental margin subduction according to the definition of [Cawood](#)
21
22 132 [et al. \(2009\)](#). Current interpretations (e.g., [Alasino et al., 2012](#)) suggest that both magmatic events
23
24 133 were linked to tectonic switching episodes in an active Pacific margin.
25
26
27
28 134
29
30 135 **3. Analytical methods**
31
32
33 136 *3.1 Geochronology*
34
35 137 Samples chosen for U–Pb zircon geochronology were prepared and analysed at the School Earth
36
37 138 and Environmental Sciences (SEES), Washington State University (WSU). As were crushed and
38
39 139 pulverized using a jaw crusher and disc mill followed by heavy mineral concentration using a
40
41 140 Gemini table. Additional density separation was carried out using methylene iodide and magnetic
42
43 141 separation using a Franz magnetic separator. Zircons (> 90% pure) were mounted in epoxy within
44
45 142 2.5 cm diameter rings, polished to expose zircon interiors, and imaged with a Scanning Electron
46
47 143 Microscope in cathode-luminescence (CL) mode at the University of Idaho.
48
49
50 144 All LA-ICP-MS U–Pb analyses were conducted at Washington State University using a New
51
52 145 Wave Nd:YAG UV 213-nm laser coupled to a ThermoFinnigan Element 2 single collector, double-
53
54
55 146 focusing, magnetic sector ICP-MS. Operating procedures and parameters are discussed in greater
56
57 147 depth by [Gaschnig et al. \(2010\)](#) and [Chang et al. \(2006\)](#) and are only briefly outlined here. Laser spot
58
59
60 148
61
62
63
64
65

size and repetition rate were 30 μm and 10 Hz, respectively. He and Ar carrier gases delivered the sample aerosol to the plasma. Time-independent (or static) fractionation is the largest source of uncertainty in LA-ICP-MS U-Pb geochronology and results from mass and elemental static fractionation in the plasma and also poorly understood laser-matrix effects (Kosler and Sylvester, 2003). It is corrected by normalizing U/Pb and Pb/Pb ratios of the unknowns to the zircon standards (Chang et al., 2006). For this study we used two zircon standards: Peixe, with an age of 564 Ma (Dickinson and Gehrels, 2003), and FC-1, with an age of 1,099 Ma (Paces and Miller, 1993).

Results are summarized in Table 1 and full data are given in Table 2 (we suggest Table 2 as Electronic Appendix 1).

3.2 Hf Isotope Analysis

In-situ LA-MC-ICP-MS Hf isotope analyses were conducted at WSU using a New Wave 213 nm UP Nd:YAG laser coupled to a Thermo-Finnigan Neptune MC-ICP-MS with 9 Faraday collectors. The laser was operated at a pulse rate of 10 Hz and power density of 10-12 J/cm² with a spot size of 40 μm , except in a few cases where smaller grains and narrower zones required a smaller spot size of 30 μm . The carrier gas consisted of purified He with small quantities of N₂ to minimize oxide formation and increase sensitivity. Analyses consisted of 60 one-second measurements in static mode.

The greatest obstacle in LA-MC-ICP-MS Hf isotopic analysis is the isobaric interference of ¹⁷⁶Yb and ¹⁷⁶Lu on ¹⁷⁶Hf (e.g., Woodhead et al., 2004). Despite the extremely low Lu/Hf in zircon, ¹⁷⁶Yb can comprise more than 10% of the total signal at mass 176 and provides the largest source of uncertainty in the measurement. A partly empirical approach was used to correct for the Yb interference, in which a modified Yb isotopic composition was calculated with Yb mass bias determined by the relationship $\beta_{\text{Yb}} = x^* \beta_{\text{Hf}}$. The value for x was determined by analyzing the zircon standards 91500, FC1, Peixe, GJ1, Mudtank, R33, Pleisovice, QGNG, and Temora and adjusting the

1
2
3 x value to best fit the known $^{176}\text{Hf}/^{177}\text{Hf}$ values previously determined on chemically purified
4
5 solutions. The x value and modified $^{176}\text{Yb}/^{173}\text{Yb}$ were then used to calculate the Hf isotopic
6
7 composition of the unknowns.
8
9

10
11 Due to the difficulty in correcting for the Yb interference and other sources of error such as
12
13 instrumental bias and matrix effects, the internal measurement error by itself is often considerably
14
15 less than the total uncertainty, which is often difficult to estimate. Based on the deviation of
16
17 $^{176}\text{Hf}/^{177}\text{Hf}$ values determined by the in situ method on the standards from the values determined by
18
19 solution analysis, the total uncertainty for individual analyses is approximately $\pm 3 \sigma$ units.
20
21
22

23 Present day and initial ε_{Hf} values were calculated using CHUR compositions of $^{176}\text{Hf}/^{177}\text{Hf}_{\text{today}} =$
24
25 0.282785 and $^{176}\text{Lu}/^{177}\text{Hf} = 0.0336$ ([Bouvier et al., 2008](#)) and a ^{176}Lu decay constant of 1.867e-11
26
27 ([Scherer et al., 2001; Söderlund et al., 2004](#)). The initial $^{176}\text{Hf}/^{177}\text{Hf}$ at the time of zircon
28
29 crystallization were used to calculate the hypothetical present-day $^{176}\text{Hf}/^{177}\text{Hf}$ of the zircons' parent
30
31 rock based on an average crustal $^{176}\text{Lu}/^{177}\text{Hf}$ of 0.015 ([Goodge and Vervoort, 2006](#)). The present day
32
33 $^{176}\text{Hf}/^{177}\text{Hf}$ and assumed rock $^{176}\text{Lu}/^{177}\text{Hf}$ values were then used to calculate a traditional TDM using
34
35 the equation: $(1/\bar{\epsilon}) * \ln[(^{176}\text{Hf}/^{177}\text{Hf} (\text{sample}) - ^{176}\text{Hf}/^{177}\text{Hf} (\text{DM})) / (^{176}\text{Lu}/^{177}\text{Hf} (\text{average crust}) -$
36
37 $^{176}\text{Lu}/^{177}\text{Hf} (\text{DM}))]$. For the depleted mantle parameters, $^{176}\text{Hf}/^{177}\text{Hf} (\text{DM}) = 0.283225$ and $^{176}\text{Lu}/^{177}\text{Hf}$
38
39 $(\text{DM}) = 0.038512$ ([Vervoort and Blichert-Toft, 1999](#)).
40
41
42
43
44

45 3.3 Sm-Nd Isotope Analysis 46

47
48 Sm–Nd determinations of representative dated granitic samples with Hf isotope zircon data were
49
50 carried out at Washington State University. For Nd whole-rock isotopic analyses, ~ 0.25 g aliquots of
51
52 whole-rock powders were dissolved at high pressure in sealed, steel-jacketed Teflon bombs with a
53
54 10:1 mixture of concentrated HF and HNO_3 acids at 150°C for 5 to 7 days. After conversion from
55
56 fluorides to chlorides, samples were spiked with a mixed $^{149}\text{Sm}-^{150}\text{Nd}$ tracer. LREE were initially
57
58 separated on cation exchange columns using AG 50W-X8 (200-400 mesh) resins; Nd and Sm were
59
60 separated on cation exchange columns using AG 50W-X8 (200-400 mesh) resins; Nd and Sm were
61
62
63
64
65

1
2
3 196 then separated from the LREE aliquot on columns with HDEHP-coated Teflon powder and HCl
4
5
6 197 ([Vervoort and Blichert-Toft, 1999](#)).
7

8 198 All analyses were conducted on a Thermo-Finnigan Neptune MC-ICP-MS. Nd analyses were
9
10 199 corrected for mass fractionation using $^{146}\text{Nd}/^{144}\text{Nd} = 0.7219$ and normalized using Ames and La Jolla
11
12 200 Nd standards. Sm analyses were corrected for fractionation using $^{147}\text{Sm}/^{152}\text{Sm} = 0.56081$. All mass
13
14 201 fractionation corrections were performed using an exponential law.
15
16

17
18 202 The uncertainties on Nd isotopic measurements reflect in-run error only and are presented as two
19
20 203 standard errors as reported by [Bouvier et al. \(2008, Table 2\)](#). The full uncertainties are better
21
22 204 assessed from the reproducibility of the standards. Average reproducibility (2 standard deviations) of
23
24 205 $^{143}\text{Nd}/^{144}\text{Nd}$ on Ames standard during the period of analysis was ± 0.000020 .
25
26

27
28 206 The decay constants used in the calculations are the values $\lambda^{147}\text{Sm} = 6.54 \times 10^{-12} \text{ year}^{-1}$
29
30 207 recommended by the IUGS Subcommission for Geochronology ([Steiger and Jaeger, 1977](#)). Epsilon-
31
32 208 Nd (ϵ_{Nd}) values were calculated relative to a CHUR: $(^{143}\text{Nd}/^{144}\text{Nd})_{\text{today}}\text{CHUR} = 0.512638$;
33
34 209 $(^{143}\text{Sm}/^{144}\text{Nd})_{\text{today}}\text{CHUR} = 0.1967$ (Goldstein et al., 1984; Jacobsen and Wasserburg, 1980). T_{DM} was
35
36 210 calculated according to [DePaolo et al. \(1991\)](#).
37
38

39
40 211 The results are reported in [Table 4](#), together with published (and in some cases recalculated) data
41
42 212 for other samples selected for Nd isotope analysis, as well as representative equivalent samples from
43
44 213 the same igneous bodies.
45
46

47
48 214 *3.4 Geochemistry*
49

50 215 Whole-rock major elements were determined for three igneous samples at the Washington State
51
52 216 University GeoAnalytical Lab, using a ThermoARL sequential X-ray fluorescence spectrometer,
53
54 217 following the procedure described by [Johnson et al. \(1999\)](#). Trace elements were determined in the
55
56 218 same samples using ICP-MS, following the procedure described in
57
58 219 <http://www.sees.wsu.edu/Geolab/note/icpms.html>.
59
60

1
2
3 Additionally, whole-rock major and trace element compositions for two samples were determined
4 at Activation Laboratories, Ontario, Canada (ACTLABS), following the 4-Lithoresearch procedure.
5
6 Following lithium metaborate/tetraborate fusion samples are dissolved in a weak nitric acid solution.
7
8 Major elements, Be, Sc, V, Sr, Ba, and Zr are determined by Inductively Coupled Plasma – Optical
9 Emission Spectroscopy (ICP-OES). All other trace elements are determined by Inductively Coupled
10 Plasma – Mass Spectrometry (ICP-MS). For major elements precision and accuracy are generally
11 better than 2% (relative). For trace elements precision and accuracy are generally better than +/- 6%
12 for all elements determined at 10 times above background.

23 4. U-Pb Geochronology

24
25 We investigated granitic rock samples that could be clearly assigned to each of the three groups
26 (i.e., Early-Middle Ordovician, Middle-Late Devonian, and Early Carboniferous ages), based on U–
27 Pb zircon ages (previously published SHRIMP data and new LA-ICP-MS analysis in this study).
28
29 Sample locations as well as the ages are summarized in [Table 1](#) and [Fig. 1](#). Full geochronological
30 data including U-Pb zircon Laser Inductively Coupled Plasma – Mass Spectrometry (LA-ICP-MS)
31
32 ages of 13 granitic rocks are found in [Table 2](#).

33 5. Hf in zircon and whole-rock Nd isotope data

34
35 Hf isotopes were determined from the magmatic growth rim zone of 14 zircons ([Table 3a, b](#) and
36 summarized in [Table 1](#), [we suggest Table 3b as Electronic Appendix 2](#)) of which had been first dated
37 by LA-ICP-MS U-Pb isotope analysis ([Table 2](#)). Only zircon areas shown to have crystallized during
38 the primary magmatic event were analysed for Hf isotopes. Inherited core zircon ages in Famatinian
39 granitic rocks define mainly Mesoproterozoic-early Neoproterozoic (ca. 1150-850 Ma) and
40 Neoproterozoic –early Cambrian (ca. 720-530 Ma) populations (data from [Ducea et al., 2010](#)), and

1
2
3
4 inherited zircons with Ordovician ages have been reported from Carboniferous plutons by Grosse et
5
6 al. (2009) and Fogliata et al. (2012). Whole-rock chemistry of the rocks with Hf and Nd isotopes data
7
8 is reported in Table 5 (we suggest Table 5 as Electronic Appendix 3). Chemical data are not
9
10 discussed here, but they are included as complementary information for those rocks with Hf and Nd
11
12 isotope data.

13
14
15 The ϵ_{Hf} values for magmatic zircons are plotted as a function of the corresponding whole-rock Nd
16
17 isotope composition at the time of crystallization ($\epsilon_{\text{Nd}_{\text{dt}}}$) and also as a function of crystallization age
18
19 (Table 3a, 5 and Fig. 2). As in the general study reported by Kemp et al. (2007), an important feature
20
21 of the Hf isotope data is the significant range of ϵ_{Hf} values exhibited by zircons within the same
22
23 sample (up to 10 ϵ units). Such variations can only be reconciled by the operation of open system
24
25 processes that are capable of changing the $^{176}\text{Hf}/^{177}\text{Hf}$ ratio of the melt from which the zircons
26
27 precipitated. Considering the scale of our work, where the objective is to evaluate the predominant
28
29 Hf isotopic compositions of the magma sources, we have selected what we consider to be the most
30
31 representative values for each sample, eliminating ‘extreme’ values (compare Table 3a and 3b) that
32
33 diverge by more than $\sim 3 \epsilon_{\text{Hf}}$ units (i.e., the total uncertainty estimated for individual analyses, see
34
35 Section 3), with exception of FAM-7086 and VEL-6017 (see explanation below). In some cases no
36
37 such filtering was necessary (Table 3a, b). However, extreme values observed in some samples
38
39 (Table 3b) are taken into account in this study because they could represent variability in the main
40
41 magma source (e.g., juvenile material contribution, deep metasediments, pre-existing crystalline
42
43 basement) or contaminants (e.g., upper crustal wall-rocks).

44
45 The Early-Middle Ordovician magmatism is by far the most voluminous of the Sierras Pampeanas
46
47 (Fig. 1) and is thus highly significant for crustal evolution in this region. These granitic rocks are
48
49 calc-alkaline (composition in Table 5) and represent an active continental margin. For these samples
50
51 ϵ_{Hf} and $\epsilon_{\text{Nd}_{\text{dt}}}$ values range from -3.3 to -14.7 and -3.3 to -6.3, respectively, with average T_{DM} Hf and

1
2
3 268 T_{DM} Nd ranging from 1.5 to 2.2 Ga and 1.4 to 1.7 Ga, respectively (Tables 1, 3a, 4 and Fig. 2). In
4 particular, sample FAM-7086 has very low zircon ϵ_{Hf} and whole-rock ϵ_{Nd} values, indicating
5
6 269 probable derivation from a Precambrian supracrustal source. However, the more mafic rocks such as
7
8 270 SVF-577 ($\text{SiO}_2 = 42.6\%$) also have Hf and Nd isotope compositions requiring a major crustal
9 component. The average ϵ_{Nd} value (calculated with $t = 473$ Ma) for Famatinian granitoids using data
10 from Dahlquist et al. (2010) is -5.1 and T_{DM} is 1.6 Ga (Table 4). The few extreme values observed in
11
12 271 some samples of Ordovician age (ANC-11030a, FAM-7086, and SVF-577, Table 3b) do not
13 significantly change the conclusion that old continental sources were involved in Famatinian
14
15 272 magmatism, predominantly contaminated by different older continental materials with distinctive
16 isotopic signature (e.g., deep crystalline basement or upper crustal wall-rocks such as
17
18 273 metasediments).

19
20 274 During the Middle-Late Devonian, magmatism was developed in a foreland position away from
21 the orogenic front in the west (Fig. 1). F-U-REE rich A-type granites formed at this time
22
23 275 (composition in Table 5). The Achala granite, the largest batholith in the Sierras Pampeanas, is
24 discordant to country rock fabrics formed during the Cambrian (Pampean) and Ordovician
25
26 276 (Famatinian) events (Rapela et al., 2008b). It has ϵ_{Hf} and ϵ_{Nd} values ranging from -3.6 to -5.8 and
27
28 277 -4.0 to -6.5, respectively (Tables 1, 3a, 4 and Fig. 2). Isotopic data from the Achala batholith show
29
30 278 ϵ_{Nd} values of -4.0 to -6.5 (mean = -4.8, data in Table 4) for the main granitic facies (all values
31 calculated with $t = 369$ Ma). Significantly more ϵ_{Hf} negative values were observed in one sample
32
33 279 only (ACH-140, Table 3b), suggesting contamination by much older metasediments at depth.

34
35 280 The Early Carboniferous A-type granites (composition in Table 5) were intruded when the region
36 was already cratonized and occur as small scattered plutons (Fig. 1) emplaced in a dominantly
37
38 281 extensional setting, within older metamorphic and igneous rocks; many of them are aligned along a
39 large reactivated shear zone (Rapela et al., 2001; Dahlquist et al., 2010). These granites have ϵ_{Hf} and
40
41 282

$\varepsilon_{\text{Nd}_{\text{dt}}}$ values ranging from -6.7 to +2.6 and -0.5 to -3.6, respectively (Tables 1, 3a, 4 and Fig. 2). The average $\varepsilon_{\text{Nd}_{\text{dt}}}$ for Carboniferous granitoids (all values calculated with $t = 343$ Ma) using data from Dahlquist et al. (2010) is -2.3 (Tables 1 and 4). Extreme values are observed in the samples of Carboniferous age (FIA-17, HUA-12, and ZAP-33, Table 3b), suggesting variable crustal contamination. An exception is FAM-177, which has an isotopic signature that suggests juvenile material in the source (Table 3a). VEL-6017 has two contrasting isotopic compositions suggesting crustal and juvenile material in the source (Table 3a).

6. Implications for crustal growth in the proto-Andean margin of Gondwana

Zircon Hf and whole-rock Nd isotopic signatures in the Early-Middle Ordovician calc-alkaline granitic magmas were predominantly derived from pre-existing continental crust and thus represent to a large extent recycling of old crustal rocks (Fig. 2) as suggested by Pankhurst et al. (2000), Rapela et al. (2008a), and Dahlquist et al. (2008). As argued by Rapela et al. (2008a), the classical Andean model for the magmas generation, invoking strong mantle contribution (e.g., Pitcher, 1979; Wilson, 1989; Parada et al., 1999; Hervé et al., 2007; and references therein) does not seem to apply to these Ordovician calc-alkaline granites. However, this view may need a degree of modification since the recent discovery of more juvenile Nd isotope compositions in the extreme west of the Sierra de Valle Fétil (Casquet et al., submitted).

Taking into account the results reported in Section 4, the scenario showed in Fig. 3a is proposed for generation of the voluminous Ordovician calc-alkaline magmas. A suite of igneous rocks of Grenvillian age (1.2-1.3 Ga) crops out in the nearby Western Sierras Pampeanas (Rapela et al., 2010), and we suggest that such rocks could have been the main source for Famatinian magmatism. Previous U-Pb and Hf determinations on zircon from small outcrops of Famatinian metaigneous rocks in La Pampa province (U-Pb zircon SHRIMP ages ranging from ca. 476 to 466 Ma) reveal

1
2
3 similar results (Chernicoff et al., 2010), with negative ϵ_{Hf} (from -3.6 to -5.0) and average Lu-Hf two
4 stages model ages of ca. 1.7 Ga.
5

6
7 Hf and Nd data from the Achala granites suggest that these A-type granitic magmas were also
8 largely derived from the recycling of old crustal rocks (Fig. 2). Consistent with this conclusion are
9 the zircon age patterns of porphyritic granites reported by Rapela et al. (2008b), which show
10 inherited components commonly found in the Cambrian metasedimentary country rocks of the
11 batholith and therefore are a likely source component for these granites. However, Rapela et al.
12 (2008b) have suggested the Achalian granites cannot be entirely derived from a Pampean basement
13 source, as the Nd isotopic composition of the basement is well bracketed within an even more
14 'crustal' isotopic range ($\epsilon_{\text{Nd520}} = -4.5$ to -7.5; Rapela et al., 2008b). Rapela et al. (2008b, data listed in
15 Table 4) reported similar ϵ_{Nd} (-4.0) for monzogranites from the same batholith. They found rather
16 more radiogenic Nd in small-scale tonalite and leucogranites bodies ($\epsilon_{\text{Nd}} = -1.2$ to -1.9, mean = -1.6,
17 and $\epsilon_{\text{Nd}} = -1.1$ to -1.4, respectively). These minor intrusions could represent a more juvenile magma
18 contribution ascending through of hypothetical local conduits.
19

20
21 The acid-to-intermediate component in a mixture is likely to dominate the Sm-Nd composition of
22 the resultant magma due to its higher Sm and Nd contents. As reported by Kemp et al. (2007), when
23 supracrustal material is reworked by juvenile magmas the Nd isotope ratios of the resulting bulk
24 magma can camouflage the juvenile component. Conversely, the zircon can crystallize sufficiently
25 early and to retain vestiges of the original isotope signature (Kemp et al., 2007). Thus, the zircon Hf
26 data could be considered more robust in constraining the source of the Middle-Late Devonian A-type
27 magmas. The ϵ_{Hf} and ϵ_{Nd} values (Table 3a, b, 4 and Fig. 2) strongly suggest a dominant older crustal
28 component (average T_{DM} Hf and T_{DM} Nd values ranging from 1.5 to 1.6 and 1.4 to 1.6, respectively),
29 and a scenario similar to that shown in Fig. 3b is assumed for the generation of A-type magmas
30 during the Middle-Late Devonian. As noticed by Nelson (1992), high abundances of P_2O_5 (up to 3.3
31
32
33
34
35
36
37
38
39
40
41
42
43
44
45
46
47
48
49
50
51
52
53
54
55
56
57
58
59
60
61
62
63
64
65

1
2
340 wt.%) and of volatiles such as F (up to 1%) could readily explained by the involvement of sediment
4
5 in the source. Achala granites have biotite with very high F content (mean = 2.1%); they bear
6
7 unusual enclaves characterized by 89–93% biotite with high FeO/MgO ratios (mean 3.1) and 7–11%
8
9 apatite with high F contents (mean 3.5%); and they have abundant zircon and monazite together with
10
11343 scarce oxides as accessory minerals (data from [Dorais et al., 1997](#)). The modal mineralogy produces
12
13344 unusual bulk-rock compositions, including enhanced $P_2O_5 = 5.4$ wt.%, F ~ 6-7 wt.%, and very high
14
15345 $U = 181$ ppm, Zr (2,581 ppm) and $\Sigma REEs = 4,500$ ppm contents (see NPE-10 sample in [Table 5](#)).
16
17

18346 We have therefore incorporated a petrogenetic scenario involving sediment contamination ([Fig. 3b](#))
19
20
21347 following the geotectonic model discussed by [Alasino et al. \(2012\)](#) for the Late Paleozoic.
22
23348

24
25349 [Grosse et al. \(2009\)](#) and [Fogliata et al. \(2012\)](#) reported the presence of zircons with Carboniferous
26
27 crystallization ages containing inherited zircon with Ordovician ages, and they consequently invoked
28350 significant participation of Ordovician meta-granitoids in the source of the Early Carboniferous A-
29
30351 type granites. However, the Carboniferous magmas could not have been entirely derived by
31
32352 remelting of the Ordovician granites because their ϵ_{Nd} values are less negative (+0.6 to -4.8 at 323 to
33
34353 354 Ma) than those of the Famatinian granitoids of 320-360 Ma (-4.8 to -8.5, [Dahlquist et al., 2010](#)).
35
36

37354 Thus, the additional participation of an asthenospheric component is required to satisfy the ϵ_{Nd} and
38
39355 ϵ_{Hf} values calculated for the Early Carboniferous granitoids. Recently, [Alasino et al. \(2012\)](#)
40
41356 concluded that the Carboniferous granitic rocks overall show west-to-east mineralogical and isotopic
42
43357 regional zonation indicating that magma genesis involved a greater contribution of juvenile material
44
45358 of mantle character towards the west. The ϵ_{Hf} values reported here are consistent with the
46
47359 conclusions of [Alasino et al., \(2012\)](#) implying continental growth by addition of juvenile material in
48
49360 a foreland region, in particular for the Cerro La Gloria pluton with $\epsilon_{Hf} = +2.6$ ([Fig. 1](#) and [Table 3a](#)).
50
51361 Thus, a petrogenetic model similar to that of [Kemp et al. \(2007\)](#), for plutonic rocks of the Lachlan
52
53362 Fold Belt (SE Australia), invoking interaction between crust of hypothetical Ordovician and
54
55363

1
2
3 364 Mesoproterozoic ages and juvenile magmas could also be applied to the generation of Eastern Sierras
4
5
6 365 Pampeanas magmas during the Early Carboniferous ([Fig. 3c](#)).
7

8 366 A striking feature evident from the new data is that the Early-Middle Ordovician magmas from
9
10 367 which most zircons crystallized were largely derived by melting of pre-existing old crustal rocks,
11
12 368 without direct participation of the asthenospheric mantle. As noted above, the Early-Middle
13
14 369 Ordovician magmatism is by far the most voluminous magmatism in the Sierras Pampeanas ([Fig. 1](#))
15
16
17 370 and represents the main magmatic event for the crustal development in this region of the proto-
18
19
20 371 Andean margin of Gondwana. The Middle-Late Devonian magmas resulted from reworking of
21
22 372 supracrustal material in a foreland region, probably modified by a limited juvenile magma
23
24 373 contribution. The Early Carboniferous magmas resulted in part from reworking of supracrustal
25
26 374 material in a largely cratonized region, but with variably more significant proportions of juvenile
27
28 375 magmas.
29
30
31
32
33 376
34

35 377 **Acknowledgments**
36
37
38 378 Financial support was provided by PIP-01940 (CONICET), Spanish CGL2009-07984/BTE, PICT
39
40 379 1009 (FONCyT), SECyT UNLaR Exp. N° 7759/2008, PID Res. 000121 MINCyT Córdoba, and a
41
42 380 CONICET external fellowship awarded to J.A. Dahlquist for his research stay at Washington State
43
44 381 University, supervised for the Professor J. Vervoort. J.A. Dahlquist thanks Professor J. Vervoort for
45
46 382 their comments on the data, and J. Vervoort, V. Valencia, G. Hart, and C. Knaack for their assistance
47
48 383 with use of the LA-ICP-MS.
49
50
51
52 384
53
54
55 385
56
57 386
58
59
60 387
61
62
63
64
65

1
2
3 388 **References**
4
5
6 389 Aceñolaza, F.G., Miller, H., Toselli, A.J., 1996. Geología del Sistema de Famatina. In: Aceñolaza,
7
8 390 F.G., Miller, H., Toselli, A.J. (Eds.), Geología del Sistema de Famatina. Münchener Geologische
9
10 Hefte, Reihe A 19(6), 412 pp.
11
12
13 392 Alasino, P.H., Dahlquist, J.A., Pankhurst, R.J., Galindo, C., Casquet, C., Rapela, C.W., Larrovere,
14
15 393 M., Fanning, C.M., 2012. Early Carboniferous sub- to mid-alkaline magmatism in the Eastern
16
17 Sierras Pampeanas, NW Argentina: a record of crustal growth by the incorporation of mantle-
18
19 derived material in an extensional setting. Gondwana Research. [Doi:10.1016/j.gr.2011.12.011](https://doi.org/10.1016/j.gr.2011.12.011)
20
21
22
23 396 Baldo, 1992. Estudio petrológico y geoquímico de las rocas ígneas y metamórficas entre Pampa de
24
25 397 Olaen y Characato. Extremo norte de la Sierra Grande de Córdoba. República Argentina. Tesis
26
27
28 398 Doctoral, Universidad Nacional de Córdoba, (*unpublished*). pp. 305.
29
30
31 399 Bouvier, A., Vervoort, J.D., Hatchett, J.P., 2008. The Lu–Hf and Sm–Nd isotopic composition of
32
33 CHUR: Constraints from unequilibrated chondrites and implications for the bulk composition of
34
35 400 terrestrial planets. Earth and Planetary Science Letters 273, 48–57.
36
37
38 402 Casquet, C., Rapela, C.W., Pankhurst, R.J., Baldo, E.G., Galindo, C., Fanning, C.M., Dahlquist, J.A.,
39
40 403 *Submitted*. Famatinian magmatic arc, juvenile magmatism, U-Pb SHRIMP zircon dating,
41
42
43 404 Gondwana, Sierras Pampeanas. Gondwana Research Letters.
44
45 405 Cawood, P.A., 2005. Terra Australis Orogen: Rodinia breakup and development of the Pacific and
46
47 406 Iapetus margins of Gondwana during the Neoproterozoic and Paleozoic. Earth-Science Reviews
48
49
50 407 69, 249 – 279.
51
52
53 408 Cawood, P.A., Kröner, A., Collins, W.J., Kusky, T.M., Mooney, W.D. y Windley, B.F., 2009.
54
55 409 Accretionary orogens through Earth history. In: Cawood, P.A., Kröner, A., (Eds.), Geological
56
57
58 410 Society, London, Special Publications 318, 1-36.
59
60
61
62
63
64
65

- 1
2
3 411 Chang, Z., Vervoort, J. D., McClelland, W. C., and Knaack, C., 2006, U-Pb dating of zircon by LA-
4
5 412 ICP-MS: Geochemistry, Geophysics, Geosystems, 7 Q05009, 1-14.
6
7 8 413 Chernicoff, C.J., Zappettini, E.O., Santos J.O.S., Allchurch, S., McNaughton, N.J., 2010. The
9
10 11 414 southern segment of the Famatinian magmatic arc, La Pampa Province, Argentina. Gondwana
12
13 415 Research 17, 662-675.
14
15 416 Collins, W.J., 2002. Hot orogens, tectonic switching, and creation of continental crust. Geology 30,
16
17 18 417 535-538.
19
20 418 Dahlquist, J.A., 2002. Mafic microgranular enclaves: early segregation from metaluminous magma
21
22 23 419 (Sierra de Chepes), Pampean Ranges, NW Argentina. Journal of South American Earth Sciences
24
25 420 15, 643-655.
26
27
28 421 Dahlquist, J.A., Galindo, C., 2004. Geoquímica isotópica de los granitoides de la sierra de Chepes:
29
30 422 un modelo geotectónico y termal, implicancias para el orógeno famatiniano. Revista de la
31
32 33 423 Asociación Geológica Argentina 59, 57-69.
34
35 424 Dahlquist, J.A., Rapela, C.W., Baldo, E.G., 2005. Cordierite-bearing S-Type granitoids in the Sierra
36
37 425 de Chepes (Sierras Pampeanas): petrogenetic implications. Journal of South American Earth
38
39 40 426 Sciences 20, 231-251.
41
42 427 Dahlquist, J.A., Pankhurst, R.J., Rapela, C.W., Casquet, C., Fanning, C.M., Alasino, P., Baez, F.M.,
43
44 45 428 2006. The San Blas Pluton: an example of Carboniferous plutonism in the Sierras Pampeanas,
46
47 429 Argentina. Journal of South American Earth Sciences 20, 341–350.
48
49
50 430 Dahlquist, J.A., Galindo, C., Pankhurst, R.J., Rapela, C.W., Alasino, P.H., Saavedra, J., Fanning,
51
52 431 C.M., 2007. Magmatic evolution of the Peñón Rosado granite: petrogenesis of garnet-bearing
53
54 432 granitoids. Lithos 95, 177-207.
55
56
57 433 Dahlquist, J.A., Pankhurst, R.J., Rapela, C.W., Galindo, C., Alasino, P., Fanning, C.M., Saavedra, J.,
58
59 434 Baldo, E., 2008. New SHRIMP U-Pb data from the Famatina Complex: constraining Early–mid

- 1
2
3 Ordovician famatinian magmatism in the Sierras Pampeanas, Argentina. *Geologica Acta* 6, 319-
4
5
6 436 333.
7
8 437 Dahlquist, J.A., Alasino, P.H., Eby, G.N., Galindo, C., Casquet, C., 2010. Fault controlled
9
10 Carboniferous A-type magmatism in the proto-Andean foreland (Sierras Pampeanas, Argentina):
11
12
13 439 Geochemical constraints and petrogenesis. *Lithos* 115, 65-81.
14
15 440 Dahlquist, J.A., Alasino, Bello, C., *Submitted*. Origin of unusual biotite-apatite bodies, Achala
16
17 batholith, Argentina. *Journal of South American Earth Sciences*.
18
19
20 442 DePaolo, D.J., Linn, A.M., Schubert, G., 1991. The continental crustal age distribution: methods of
21
22 determining mantle separation ages from Sm–Nd isotopic data and application to the
23
24 southwestern United States. *Journal Geophysical Research* 96, 2071–2088.
25
26
27
28 445 Dickinson, W.R. & Gehrels, G.E., 2003. U-Pb ages of detrital zircons from Permian and Jurassic
29
30 446 eolian sandstones of the Colorado Plateau, USA: paleogeographic implications. *Sedimentary*
31
32
33 447 *Geology* 163, 29–66.
34
35 448 Dorais, M., Lira, R., Chen, Y., Tingey, D. 1997. Origin of biotite-apatite-rich enclaves, Achala
36
37
38 449 Batholith, Argentina. *Contributions to Mineral and Petrology* 130, 31-46.
39
40 450 Ducea, M.N., Otamendi, J.E., Bergantz, G., Stair, K.M., Valencia, V.A., Gehrels, G.E., 2010. Timing
41
42
43 451 constraints on building an intermediate plutonic arc crustal section: U- Pb zircon geochronology
44
45 452 of the Sierra Valle Fértil–La Huerta, Famatinian arc, Argentina. *Tectonics* 29, TC4002, 21-22.
46
47 453 Fogliata, A.S., Báez, M.A., Hagemann, S.G., Santos, J.O, Sardi, F., 2012. Post-orogenic,
48
49
50 454 Carboniferous granite-hosted Sn–W mineralization in the Sierras Pampeanas Orogen,
51
52
53 455 Northwestern Argentina. *Ore Geology Reviews* 45, 16-32.
54
55 456 Gaschnig, R.M., Vervoort, J.D., Lewis, R.S., McClelland, W.C., 2010. Migrating magmatism in the
56
57
58 457 northern US Cordillera: in situ U–Pb geochronology of the Idaho batholiths. *Contributions to*
59
60 458 *Mineralogy and Petrology* 159, 863-883.

- 1
2
3 459 Goldstein, S. J.; O`Nions, R.K.; Hamilton, P.J. 1984., A Sm.Nd isotopic study of atmospheric dusts
4
5
6 460 and particulates from major river systems. *Earth and Planetary Science Letters* 70, 221-
7
8 461 236.Grisson, G.C., Debari, S.M., Snee, L.W., 1998. Geology of the Sierras de Fiambalá,
9
10
11 462 northwestern Argentina: implications for Early Palaeozoic Andean tectonics. In: Pankhurst,
12
13 463 R.J., Rapela, C.W. (Eds.), *The Proto-Andean Margin of Gondwana: Journal of the Geological*
14
15 464 Society, London, Special Publications 142, 297–323.
16
17
18 465 Goodge, J. W., and Vervoort, J. D., 2006. Origin of Mesoproterozoic A-type granites in Laurentia:
19
20 466 Hf isotope evidence. *Earth and Planetary Science Letters*, 243, 711-731.
21
22
23 467 Grosse, P., Söllner, F., Baéz, M.A., Toselli, A.J., Rossi, J.N., de la Rosa, J.D., 2009. Lower
24
25 468 Carboniferous post-orogenic granites in central-eastern Sierra de Velasco, Sierras Pampeanas,
26
27
28 469 Argentina: U-Pb monazite geochronology and Sr-Nd isotopes. *International Journal of Earth*
29
30 470 *Sciences* 98, 1001-1025.
31
32
33 471 Hervé, F., Pankhurst, R.J., Fanning, C.M., Calderón, M. & Yaxley, G.M., 2007. The South
34
35 472 Patagonian batholith: 150 my of granite magmatism on a static plate margin. *Lithos* 97: 373-394.
36
37 473 Höckenreiner, M., Söllner, F., Miller, H., 2003. Dating the TIPA shear zone: an early Devonian
38
39
40 474 terrane boundary between the Famatinian and Pampean systems (NW Argentina). *Journal of South*
41
42 475 *America Earth Sciences* 16, 45-66.
43
44
45 476 Jacobsen S. B., Wasserburg G. J., 1980. Sm-Nd isotopic evolution of chondrites. *Earth and Planetary*
46
47 477 *Science Letters* 50, 139-155.
48
49
50
51 478 Johnson, D.M., Hooper P.R., Conrey, R.M., 1999. XRF analysis of rocks and minerals for major and
52
53
54 479 trace elements on a single low dilution Litetraborate fused bead. *Advances in X-ray Analysis* 41,
55
56 480 843-867.
57
58
59 481 Kemp, A.I.S., Hawkesworth, C. J., Paterson, B. A., Kinny, P.D., 2006. Episodic growth of the
60
61 482 Gondwana supercontinent from hafnium and oxygen isotopes in zircon. *Nature* 439, 580-583.
62
63
64
65

- 1
2
3 483 Kemp, A.I.S., Hawkesworth, C.J., Foster, G.L., Paterson, G.A., Woodhead, J.D., Hergt, J.M., Gray,
4
5
6 484 C.M., Whitehouse, M.J., 2007. Magmatic and crustal differentiation history of granitic rocks
7
8 485 from Hf–O isotopes in zircon. *Science* 315, 980–983.
9
10
11 486 Kosler, J. & Sylvester, P.J. 2003. Present trends and the future of zircon in geochronology: laser
12
13 487 ablation ICPMS. In: Hanchar, J.M. & Hoskin, P.W.O. (eds). *Zircon. Reviews in Mineralogy and*
14
15 488 *Geochemistry* 53, 243– 276.
16
17
18 489 Llambías, E.J., Sato, A.M., Ortiz Suárez, A., Prozzi, C., 1998. The granitoids of the Sierra de San
19
20 490 Luis. In: Pankhurst, R.J., Rapela, C.W. (Eds.), *The Proto-Andean margin of Gondwana:*
21
22
23 491 Geological Society of London, Special Publications 142, pp. 325–341.
24
25 492 López de Luchi, M.G., Rapalini, A.E., Siegesmund, S., Steenken, A. 2004. Application of magnetic
26
27 493 fabrics to the emplacement and tectonic history of Devonian granitoids in central Argentina. In:
28
29
30 494 Martín-Hernández, F., Lüneburg, F., Aubourg, C. y Jackson, M. (eds.) *Magnetic fabric: methods*
31
32
33 495 and applications, Geological Society, London, Special Publications 238: 447-474.
34
35 496 Miller, C.F., McDowell, S.M., Mapes, R.W., 2003. Hot and cold granites? Implications of zircon
36
37 497 saturation temperatures and preservation of inheritance. *Geology* 31, 529–532.
38
39
40 498 Miller, H., Söllner, F., 2005. The Famatina complex (NW-Argentina): back-docking of an island arc
41
42 499 or terrane accretion? Early Palaeozoic geodynamics at the western Gondwana margin. In:
43
44
45 500 Vaughan, A.P.M., Leat, P.T., Pankhurst, R.J. (Eds.), *Terrane processes at the margins of*
46
47 501 *Gondwana*. Geological Society of London, Special Publication 246, 241-256.
48
49
50 502 Nelson, D.R. 1992. Isotopic characteristic of potassic rocks. Evidence for the involvement of
51
52 503 subducted sediment in magma genesis. *Lithos* 28, 403-420.
53
54
55 504 Paces, J.B., and Miller, J.D. 1993, Precise U-Pb ages of Duluth Complex and related mafic
56
57 505 intrusions, north- eastern Minnesota: geochronological insights to physical, petrogenetic,
58
59
60
61
62
63
64
65

1
2
3 506 paleomagnetic, and tectonomagmatic processes associated with the 1.1 Ga midcontinental rift
4
5 507 system. *Journal Geophysical Research* 98, 13997–14013.
6
7

8 508 Pankhurst, R.J., Rapela, C.W., 1998. Theproto-AndeanmarginofGondwana: an introduction. The
9
10 proto-Andean margin of Gondwana. In: Pankhurst, R.J., Rapela, C.W. (Eds.), Geological
11 509 Society, London, Special Publications, vol. 142, pp. 1–9.
12
13 510 Pankhurst, R.J., Rapela, C.W., Fanning, C.M. 2000. Age and origin of coeval TTG, I–S-type granites
14
15 511 in the Famatinian belt of NW Argentina. *Transactions of the Royal Society of Edinburgh, Earth*
16
17 512 Sciences 91, 151–168.
18
19
20 513 Pankhurst, R.J., Rapela, C.W., Saavedra, J., Baldo, E.G., Dahlquist, J.A., Pascua, I., Fanning, C.M.,
21
22
23 514 1998. The Famatinian arc in the central Sierras Pampeanas: an Early to Mid-Ordovician
24
25 515 continental arc on the Gondwana margin. In: Pankhurst, R.J., Rapela, C.W. (Eds.), *The Proto-*
26
27 516 *Andean Margin of Gondwana*. Geological Society of London, Special Publication 142, 343-367.
28
29
30 517 Parada, M.A., Nyström, J.O., Levi, B., 1999. Multiple sources for the Coastal Batholith of central
31
32 518 Chile (31°-34°S): geochemical and Sr-Nd isotopic evidence and tectonics implications. *Lithos*
33
34 519 46, 505-521.
35
36
37 520 Pinotti, L., Coniglio, J., Esparza, A., D'Eramo, F., Llambías, E., 2002. Nearly circular plutons
38
39
40 521 emplaced by stoping at shallow crustal levels, Cerro Áspero batholith, Sierras Pampeanas de
41
42 522 Córdoba, Argentina. *Journal of South American Earth Sciences* 15, 251-265.
43
44
45 523 Pinotti, L., Tubía, J.M., D'Eramo, F., Vegas, N., Sato, A.M., Coniglio, J. y Aranguren, A., 2006.
46
47 524 Structural interplay between plutons during the construction of a batholith (Cerro Aspero
48
49 525 batholith, Sierras de Córdoba, Argentina). *Journal of Structural Geology* 28, 834-849.
50
51
52 526 Pitcher, W.S., 1979. The nature, ascent and emplacement of granitic magmas. *Journal of the*
53
54
55 527 *Geological Society, London* 136, 627-662.
56
57
58
59
60
61
62
63
64
65

- 1
2
3 529 Rapela, C.W., Pankhurst, R.J., Dahlquist, J.A., Baldo, E.G., Casquet, C., Galindo, C., 2008a.
4
5
6 530 Revisiting accretionary history and magma sources in the Southern Andes: Time variation of
7
8 531 "typical Andean granites". International Symposium on Andean Geodynamics, 7th, Nice, France,
9
10 532 extended abstracts, 427-430.
11
12
13 533 Rapela, C.W., Baldo, E.G., Pankhurst, R.J., Fanning, C.M., 2008b. The Devonian Achala batholith in
14
15 534 the Sierras Pampeanas: F-rich aluminous A-type granites. San Carlos de Bariloche, Argentina.
16
17 18 535 South American Symposium on Isotope Geology, 6th, CD-ROM, extended abstract 53.
19
20 536 Rapela, C.W., Pankhurst, R.J., Casquet, C., Baldo, E., Galindo, C., Fanning, C.M., Dahlquist, J.A.,
21
22
23 537 2010. The Western Sierras Pampeanas: Protracted Grenville-age history (1330–1030 Ma) of
24
25 538 intra-oceanic arcs, subduction–accretion at continental-edge and AMCG intraplate magmatism.
26
27
28 539 Journal of South American Earth Sciences 29, 105-127.
29
30 540 Saavedra, J., Toselli, A., Rossi, J., Pellitero, E., Durand, F., 1998. The Early Palaeozoic magmatic
31
32
33 541 record of the Famatina System: a review. In: Pankhurst, R.J., Rapela, C.W. (Eds.). The Proto-
34
35 542 Andean Margin of Gondwana. Journal of the Geological Society of London, Special Publication
36
37 543 142, 283-295.
38
39
40 544 Scherer, E., Whitehouse, M.J., Müunker, C., 2007. Zircon as a monitor of crustal growth. Elements 3,
41
42
43 545 19–24.
44
45 546 Siebel, W. & Chen, F. 2010. Zircon Hf isotope perspective on the origin of granitic rocks from
46
47 547 eastern Bavaria, SW Bohemian Massif. International Journal of Earth Sciences 99, 993–1005.
48
49
50 548 Siegesmund, S., Steenken, A., López de Luchi, M.G., Wemmer, K., Hoffmann, A., Mosch, S., 2004.
51
52
53 549 The Las Chacras–Potrerillos batholith (Pampean Ranges, Argentina): structural evidence,
54
55 550 emplacement and timing of the intrusion. International Journal Earth Sciences 93, 23–43.
56
57
58 551 Sims, J.P., Ireland, T.R., Camacho, A., Lyons, P., Pieters, P.E., Skirrow, R.G., Stuart-Smith, P.G.
59
60 552 1998. U–Pb, Th–Pb and Ar–Ar geochronology from the southern Sierras Pampeanas, Argentina:
61
62
63
64
65

1
2
3 implications for the Palaeozoic tectonic evolution of the western Gondwana margin. In:

4
5
6 Pankhurst, R.J. & Rapela, C.W. (eds) *The Proto-Andean Margin of Gondwana*. Geological

7
8 Society, London, Special Publications 142, 259-281.

9
10 Söderlund, U., Patchett, P. J., Vervoort, J. D., and Isachsen, C. E., 2004. The ^{176}Lu decay constant

11
12 determined by Lu-Hf and U-Pb isotope systematics of Precambrian mafic intrusions. *Earth*

13
14 and *Planetary Science Letters* 219, 311-324.

15
16 Spagnuolo, C.M., Rapalini, A.E., Astini, R.A., 2012. Assembly of Pampia to the SW Gondwana

17
18 margin: a case of strike-slip docking? *Gondwana Research* 21, 406-421.

19
20 Steiger, R.H., Jäger, E., 1977. Subcommission of geochronology: convention on the use of decay

21
22 constants in geo- and cosmochronology. *Earth and Planetary Science Letters* 36, 359–362.

23
24 Stuart-Smith, P.G., Miró, R., Sims, J.P., Pieters, P.E., Lyons, P., Camacho, A., Skirrow, R.G. and

25
26 Black, L.P., 1999. Uranium-lead dating of felsic magmatic cycles in the southern Sierras

27
28 Pampeanas, Argentina: implications for the tectonic development of the proto-Andean

29
30 Gondwana margin, in: V.A., Ramos, J.D., Keppie (Eds.), *Laurentia Gondwana connections*

31
32 before Pangea. *Geological Society of America Special Publication* 336, 87-114.

33
34 Tohver, E., Cawood, P.A., Rossello, E.A., Jourdan, F., 2012. Closure of the Clymene Ocean and

35
36 formation of West Gondwana in the Cambrian: evidence from the Sierras Australes of the

37
38 southernmost Rio de la Plata craton, Argentina. *Gondwana Research* 21, 394-405.

39 Vaughan, A.P.M., Pankhurst, R.J., 2008. Tectonic overview of the West Gondwana margin.

40
41
42 Gondwana Research 13, 150–162.

43
44 Vervoort, J.D. & Blichert-Toft, J., 1999. Evolution of the depleted mantle: Hf isotope evidence from

45
46 juvenile rocks through time. *Geochimica et Cosmochimica Acta* 63, 533-556.

47
48 Wedepohl, K.H., 1995. The composition of the continental crust: *Geochimica et Cosmochimica Acta*

49
50
51
52
53
54
55
56
57
58
59
60
61
62
63
64
65

576 59, 1217-1232.

1
2
3 577 Wilson, M. 1989. Igneous Petrogenesis, A Global Tectonic Approach. Unwin Hyman, London. pp.
4
5
6 578 466.
7

8 579 Willner, A.P., Gerdes, A., Massonne, H.-J., Schmidt, A., Sudo, M., Thomson, S.N., Vujovich, G.,
9
10
11 580 2011. The geodynamics of collision of a microplate (Chilenia) in Devonian times deduced by
12
13 581 the pressure–temperature–time evolution within part of a collisional belt (Guarguaraz
14
15 582 complex, W-Argentina). Contributions to Mineralogy and Petrology 162, 303–327.
16
17
18 583 Woodhead, J., Hergt, J., Shelley, M., Eggins, S., Kemp, R. 2004. Zircon Hf-isotope analysis with an
19
20 584 excimer laser, depth profiling, ablation of complex geometries, and concomitant age estimation.
21
22
23 585 Chemical Geology 209, 121–135.
24
25 586
26
27
28 587
29
30 588
31
32
33 589
34
35 590
36
37
38 591
39
40 592
41
42
43 593
44
45 594
46
47
48 595
49
50 596
51
52 597
53
54
55 598
56
57 599
58
59
60 600
61
62
63
64
65

FIGURE CAPTIONS

Fig. 1. Simplified geological map of central-west Argentina (Sierras Pampeanas), central Chile, and the location of the studied Early-Middle Ordovician calc-alkaline granites and Middle-Late Devonian (Achala batholith) and Early Carboniferous A-type granites. Coupled in situ U-Pb ages and Hf isotope data for zircons and whole-rock Sm/Nd data are included. Sources: *U-Pb zircon SHRIMP ([Pankhurst et al., 2000](#)); †N.D. = Not determined; §U-Pb zircon SHRIMP ([Alasino et al., 2012](#)); **U-Pb zircon SHRIMP (Rapela et al. 2008b), otherwise data reported in this paper. Inset: Schematic geological map of South America showing the location of Sierras Pampeanas in Argentina.

Fig. 2. (a) The average Hf isotope composition of melt-precipitated zircons from samples of each suite as a function of whole-rock Nd isotope composition at the time of crystallization of the granitic rocks of Sierras Pampeanas. **(b)** ϵ_{Hft} values for magmatic zircons are plotted as a function of crystallization age. VEL-6017 defines two Hf compositions populations (see text). The depleted mantle evolution curve is from [Kemp et al. \(2006\)](#).

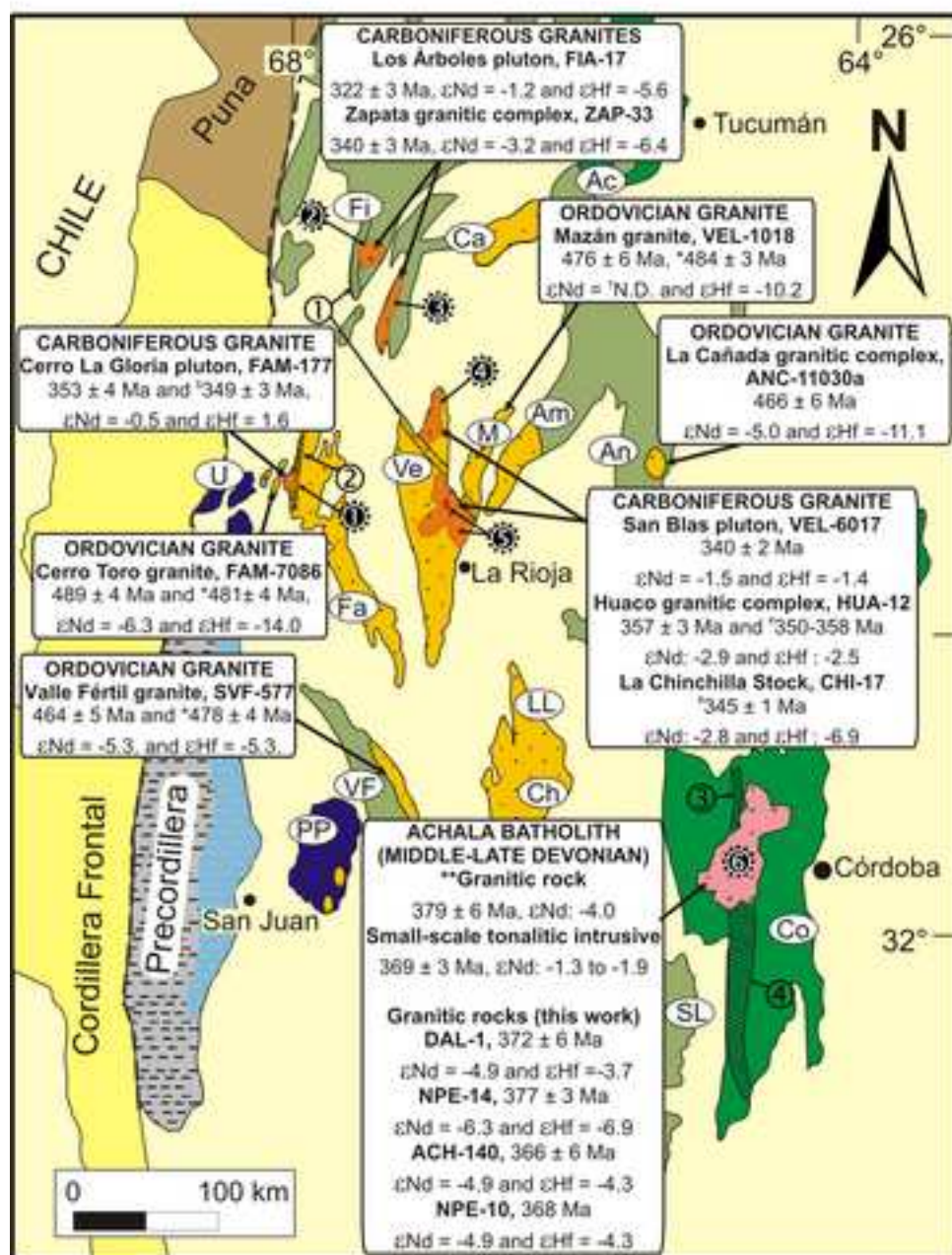
Fig. 3. Upper figure: Possible schematic geodynamic scenario for magma generation in the proto-Andean margin of Gondwana at between 32° and 26°S (see [Fig. 1](#)). **Lower figure:** Cartoon of the standard profile of the continental crust, modified from [Wedepohl \(1995\)](#). Generalized location for each magmatic event in [Fig. 1](#): **(a)** Early-Middle Ordovician magma generation in a roll-back subduction setting, **(b)** Middle-Late Devonian and **(c)** Early Carboniferous magma generation in a dominant extensional regime with subsequent lithosphere thinning. The final emplacement of Achala granites is in dominant compressional regimen (see discussion in the

1
2
3 text). The ascent of magmas during the Early Carboniferous (and probably during the Middle-
4
5 Late Devonian) was facilitated by shear zones (see discussion in the text). The probable source
6 for each setting is: **(a)** Early-Middle Ordovician: Mesoproterozoic continental crust (T_{DM} Hf =
7 1.5-2.2 Ga and T_{DM} Nd = 1.4-1.7 Ga), with no significant asthenospheric mantle contribution;
8 **(b)** Middle-Late Devonian and **(c)** Early Carboniferous: mainly the Sierra de Córdoba basement
9 and Ordovician granites, respectively. **(b)** and **(c)** support Mesoproterozoic continental crust
10 source (see T_{DM} Hf and T_{DM} Nd in [Table 3a](#), [b](#) and [5](#)) and a progressive mantle contribution (see
11 discussion in the text). The presence of paleo-sediment in the source for settings **(b)** and **(c)** was
12 included in agreement with the geotectonic scenario discussed by [Alasino et al. \(2012\)](#).
13
14
15
16
17
18
19
20
21
22
23
24
25
26
27
28
29
30
31
32
33
34
35
36
37
38
39
40
41
42
43
44
45
46
47
48
49
50
51
52
53
54
55
56
57
58
59
60
61
62
63
64
65 References for the three figures in [Fig. 3a](#).

Figure

[Click here to download high resolution image](#)

Fig. 1

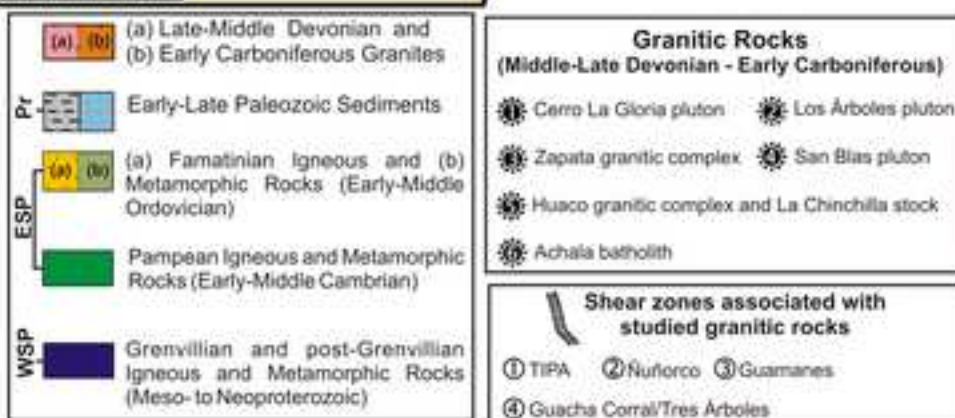


REFERENCES

Mountain ranges

Pr: Precordillera
ESP: Eastern Sierras Pampeanas
WSP: Western Sierras Pampeanas

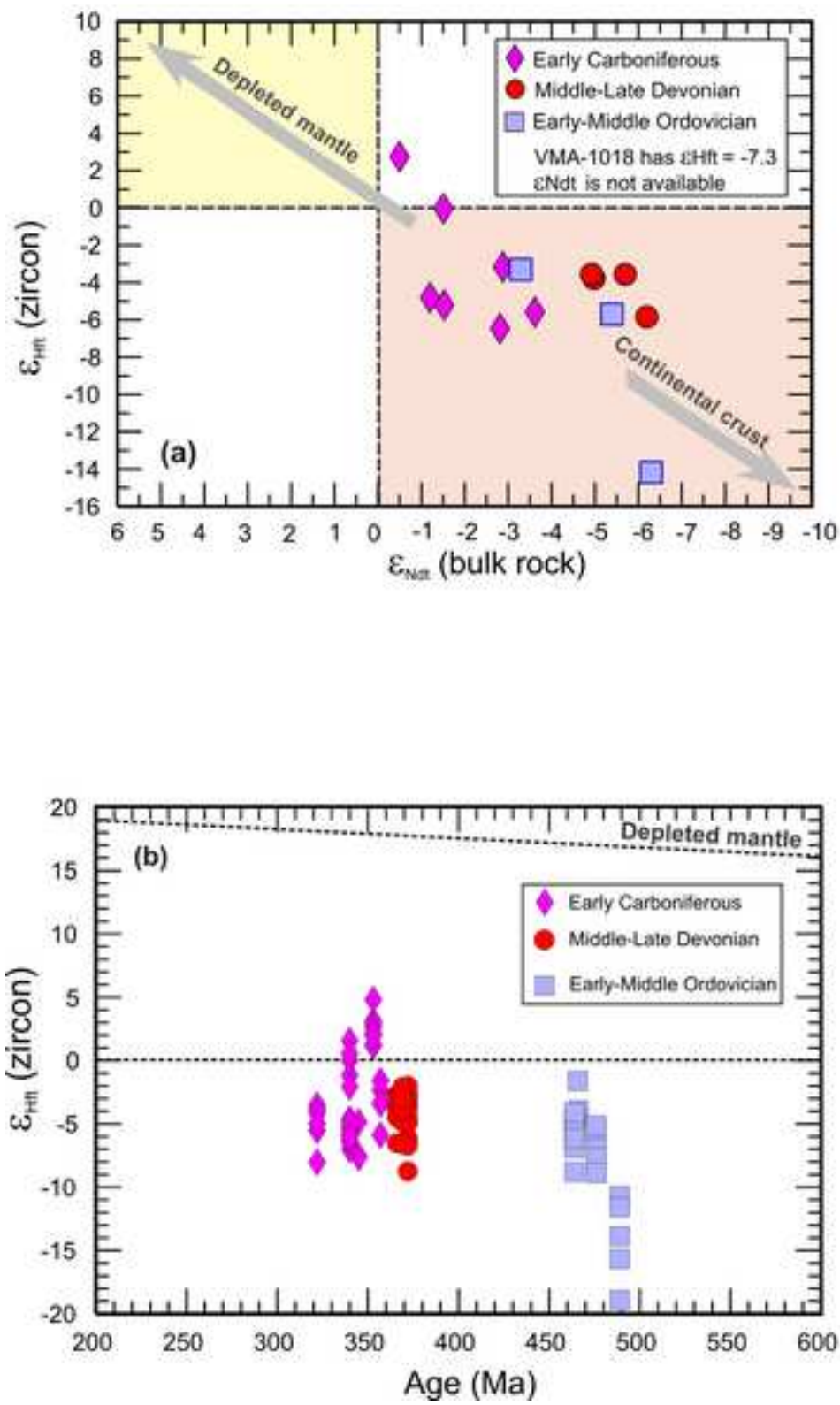
Ac: Aconquija; Am: Ambato; An: Ancasti; M: Mazán; Ca: Capilla; Co: Córdoba; Ch: Chepes; Fa: Famatina; Fi: Fiambalá; Ve: Velasco; LL: Los Llanos; VF: Valle Fértil; PP: Pie de Palo; SL: San Luis; U: Umango.



Figure

[Click here to download high resolution image](#)

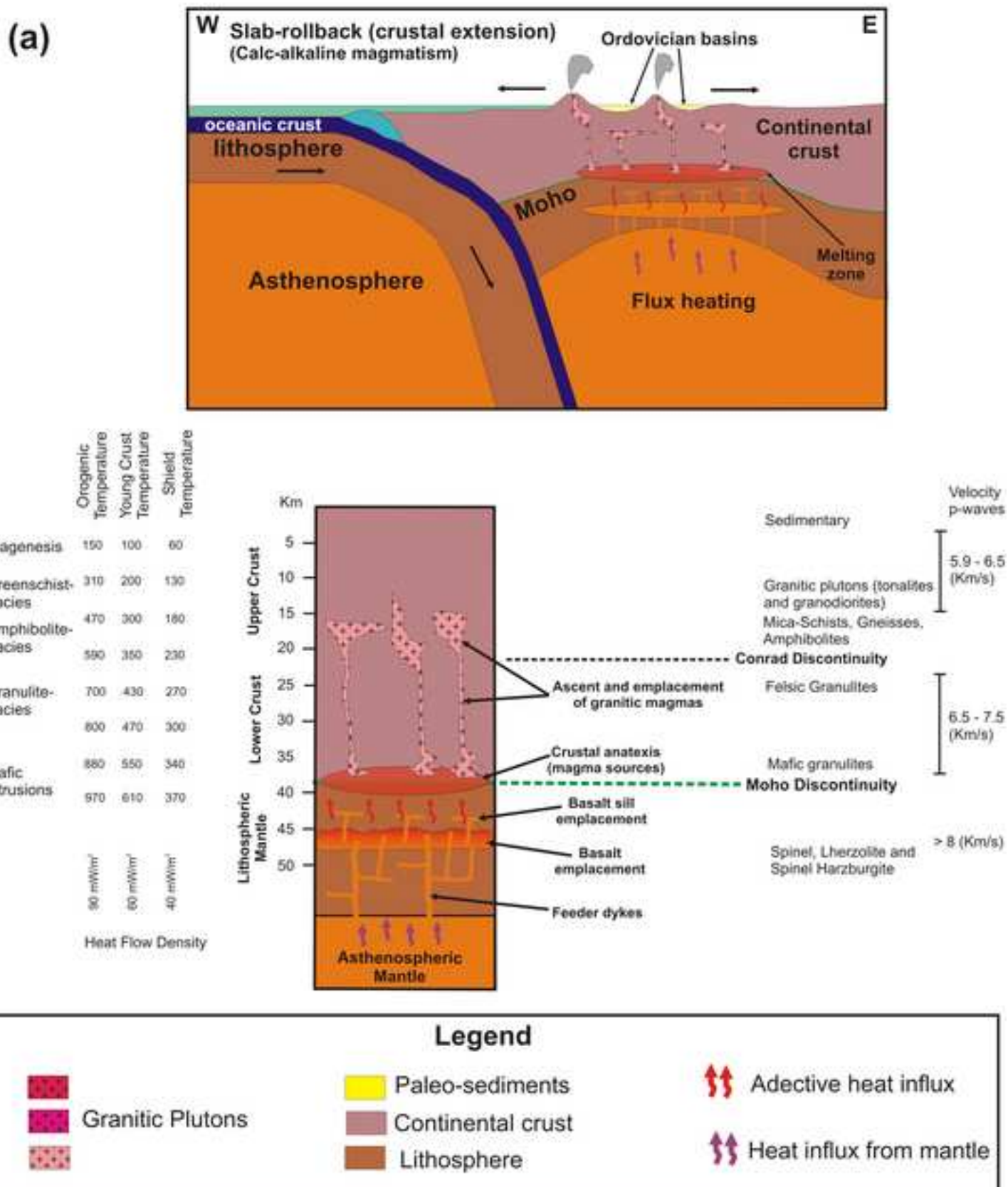
Fig. 2



Figure

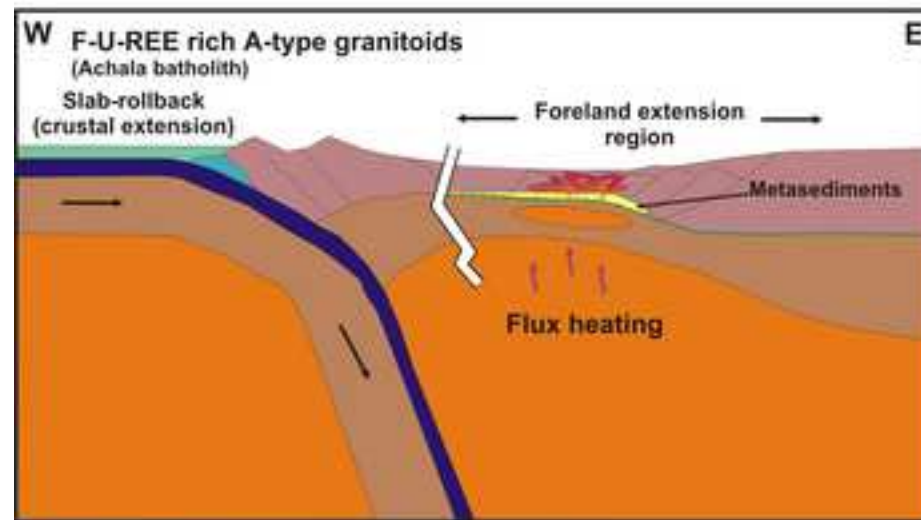
[Click here to download high resolution image](#)

Fig. 3a



Figure

[Click here to download high resolution image](#)



(b)

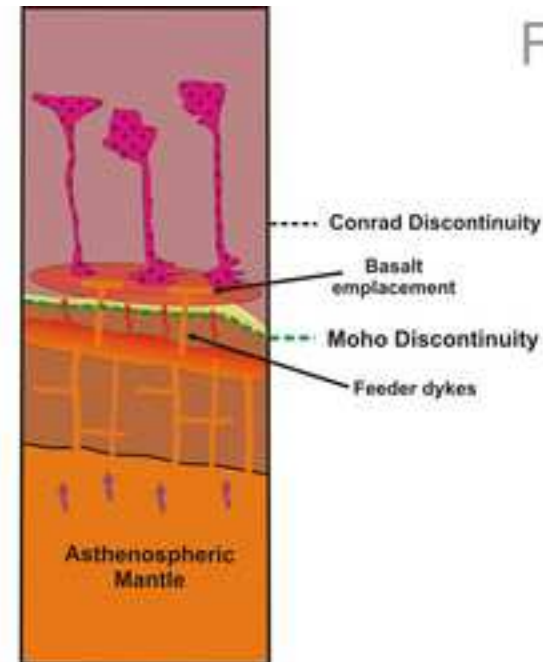
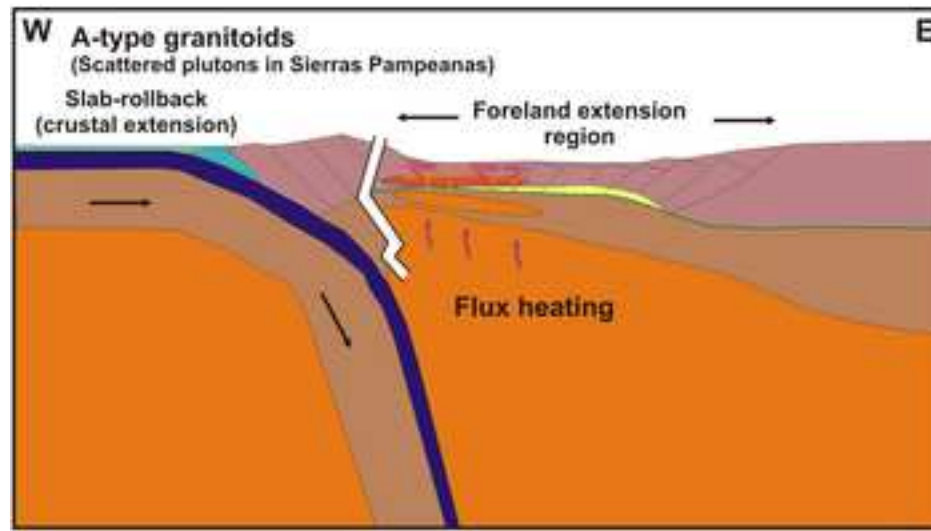


Fig. 3b, c



(c)

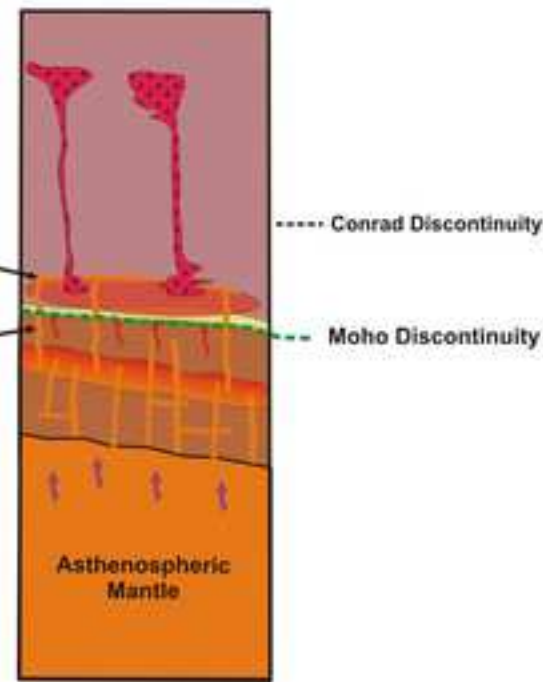


Table 1.

Integrated in situ U-Pb and Hf isotopes in zircon and whole-rock and isotopes data for the studied rocks (see Fig. 1)

	U-Pb Ages*	U-Pb Ages†	ε Nd(t)‡	ε Hf(t)	T _{DM} Nd	T _{DM} Hf	Latitude	Longitude
<i>Early-Middle Ordovician granitic rocks</i>								
<i>Samples</i>								
SVF-577	464 ± 5	478 ± 4	-5.4	-5.7	1.6	1.7	30° 39' 28"	67° 36' 17"
VMA-1018	476 ± 6	484 ± 3	N.D.‡	-7.3	N.D.	1.8	28° 43' 31"	66° 34' 31"
FAM-7086	483 ± 8	481 ± 4	-5.9	-14.7	1.7	2.2	29° 01' 25"	68° 10' 19"
ANC-11030a	466 ± 6	N.D.	-4.9	-3.3	1.6	1.5	28° 57' 56"	65° 25' 08"
<i>Middle-Late Devonian granitic rocks</i>								
ACH-140	366 ± 6	N.D.	-5.0	-3.8	1.5	1.5	31° 36' 37"	64° 49' 49"
DAL-1	372 ± 6	N.D.	-4.9	-3.6	1.5	1.5	31° 25' 50"	64° 53' 00"
NPE-14	369 ± 5	N.D.	-6.3	-5.9	1.6	1.6	31° 26' 02"	64° 49' 29"
NPE-10	369**	N.D.	-5.7	-3.8	1.6	1.5	31° 25' 46"	64° 49' 50"
<i>Early Carboniferous granitic rocks</i>								
FIA-17 (Los Árboles pluton)	322 ± 3		-1.6	-5.0	1.2	1.6	27° 44' 31"	67° 30' 04"
VEL-6017 (San Blas pluton)	340 ± 2	340 ± 3	-1.6	-5.2 and +0.5	1.2	1.6 and 1.3	28° 27' 14"	67° 06' 02"
ZAP-33 (Zapata granitic complex)	332 ± 3		-3.6	-5.8	1.4	1.6	27° 53' 18"	67° 21' 15"
FAM-177 (Cerro La Gloria pluton)	353 ± 4	349 ± 3††	-0.5	2.6	1.2	1.1	29° 04' 57.1"	67° 57' 03.9"
HUA-12 (Huaco granitic complex)	357 ± 3		-2.9	-3.3	1.3	1.5	29° 11' 23"	67° 01' 45"
CHI-17 (La Chinchilla stock)	345 ± 1§§		-2.8	-6.7	1.3	1.7	29° 10' 09"	66° 58' 20"

NOTE: Compilation of data from Tables 3 and 4. VMA-1018 is not available for Sm/Nd determinations. VEL-6017 defines two Hf compositions populations (see Table 3).

*U-Pb zircon LA-ICP-MS, this work.

†U-Pb zircon SHRIMP (Pankhurst et al., 2000; Dahlquist et al., 2008).

‡t = 473, data from Table 4.

#N.D. = not determined.

**Average from ACH-140, DAL-1, and NPE-14. An U-Pb zircon age = 368 Ma was obtained by Dorais et al. (1997) for a rock such as NPE-10.

††U-Pb zircon SHRIMP from Alasino et al. (2012).

§§U-Pb monazite LA-ICP-MS from Grosse et al. (2009).

Table**Table 2 Electronic Appendix 1.**

LA-ICP-MS zircon results for the biotite-bearing tonalite of the Las Cañas granitic complex.

Grain spot	^{238}U ^{206}Pb	1σ	^{207}Pb ^{206}Pb	1σ	$^{206}\text{Pb}/^{238}\text{U}$	1σ	$^{207}\text{Pb}/^{206}\text{Pb}$	1σ
ANC 11030a (P)								
ANC-11030a_2a*	13.369	0.405	0.05630	0.00083	465	14	464	32
ANC-11030a_4b	13.680	0.415	0.06035	0.00075	455	13	616	26
ANC-11030a_5a*	13.530	0.411	0.05637	0.00071	460	13	467	28
ANC-11030a_7a	13.146	0.305	0.05803	0.00037	473	11	455	15
ANC-11030a_9a	12.805	0.292	0.05728	0.00083	485	11	531	14
ANC-11030a_16a	13.727	0.318	0.06206	0.00086	453	10	502	31
ANC-11030a_19a	13.658	0.252	0.05690	0.00081	456	8	676	29
ANC-11030a_24a*	13.215	0.279	0.05663	0.00076	470	10	488	31
ANC-11030a_25a*	13.438	0.203	0.05690	0.00079	463	7	477	30
ANC-11030a_27a	13.689	0.201	0.05690	0.00079	455	6	488	31
ANC-11030a_8a	13.339	0.269	0.05712	0.00047	467	11	496	18
ANC 11030a (F)								
ANC-11030a_2a *	13.344	0.206	0.05601	0.00032	466	7	453	13
ANC-11030a_5a *	13.505	0.209	0.05608	0.00024	461	7	456	10
ANC-11030a_7a *	13.170	0.117	0.05638	0.00029	472	4	467	11
ANC-11030a_8a *	13.339	0.135	0.05744	0.00033	466	5	509	12
ANC-11030a_9a	12.828	0.111	0.05836	0.00030	484	4	543	11
ANC-11030a_24a *	13.209	0.118	0.05667	0.00034	470	4	479	13
ANC-11030a_25a *	13.432	0.068	0.05640	0.00031	463	2	468	12
ANC-11030a_1a	6.640	0.106	0.07075	0.00032	904	14	950	9
ANC-11030a_17a	11.720	0.082	0.05940	0.00035	528	4	582	13
ANC-11030a_18a	2.383	0.106	0.11516	0.00127	2258	84	1882	20

NOTE (all Tables): 1. $^{238}\text{U}/^{206}\text{Pb}$ ratio corrected for static fractionation using Peixe (P) and FC1 (F), respectively. 2. Measurement errors represent within-run standard error uncertainty only. 3. $^{207}\text{Pb}/^{206}\text{Pb}$ ratios corrected for static fractionation using Peixe (P) and FC1 (F), respectively. 4. Asterisk (*) indicates data points used for Concordia age calculation. 5. In red color the ages used in the calculations of epsilon Nd and Hf, respectively. 6. Localization of samples in Fig. 1 and Table 1.

[†]Previous age (LA-ICP-MS U-Pb in zircon) reported by Dahlquist et al. (2012).

Concordia Age = 465 ± 5 Ma
(2σ , decay-const. errs included)
MSWD (of concordance) = 1.3,
Probability (of concordance) = 0.26

Concordia Age = 466 ± 5 Ma[†]
(95% confidence, decay-const. errs included)
MSWD (of concordance) = 0.52,
Probability (of concordance) = 0.47

Table 2

LA-ICP-MS Zircon results for the gabbro of the Sierra de Valle Fértil.

Grain	^{238}U	1σ	^{207}Pb	1σ	$^{206}\text{Pb}/^{238}\text{U}$	1σ	$^{207}\text{Pb}/^{206}\text{Pb}$	1σ
spot	^{206}Pb		^{206}Pb		age		age	
SVF-577 (P)								
Grain 1	13.355	0.200	0.05669	0.00078	465	7	474	21
Grain 4	13.309	0.196	0.05646	0.00070	467	7	489	19
Grain 5*	12.808	0.190	0.05712	0.00071	485	7	484	18
Grain 6*	12.798	0.188	0.05662	0.00071	485	7	487	18
Grain 7*	12.964	0.189	0.05577	0.00070	479	7	488	18
Grain 8*	13.642	0.230	0.05802	0.00092	456	7	890	33
Grain 9	13.409	0.187	0.05636	0.00074	464	6	464	21
Grain 10*	13.092	0.194	0.05934	0.00090	475	7	591	24
Grain 12*	13.363	0.371	0.05880	0.00062	465	12	948	39
Grain 13	13.666	0.353	0.05677	0.00044	455	11	466	15
Grain 14*	12.889	0.340	0.05614	0.00050	482	12	471	17
Grain 16	13.139	0.127	0.05598	0.00048	473	4	482	18
Grain 18*	13.389	0.132	0.05549	0.00060	464	4	452	23
Grain 19	13.281	0.117	0.05619	0.00041	468	4	487	15
Grain 20*	12.655	0.138	0.05807	0.00061	490	5	552	25
SVF-577 (F)								
Grain 1	13.450	0.327	0.05670	0.00053	462	11	474	21
Grain 4	13.403	0.324	0.05647	0.00040	464	11	489	19
Grain 5*	12.898	0.313	0.05713	0.00041	481	11	484	18
Grain 6*	12.888	0.311	0.05662	0.00042	482	11	487	18
Grain 7*	13.055	0.314	0.05578	0.00042	476	11	488	18
Grain 8*	13.738	0.351	0.05803	0.00070	453	11	890	33
Grain 9*	13.503	0.320	0.05637	0.00047	461	11	464	21
Grain 10*	13.184	0.319	0.05935	0.00067	471	11	591	24
Grain 12*	13.029	0.920	0.05855	0.00062	477	32	948	39
Grain 13	13.325	0.932	0.05652	0.00043	466	31	466	15
Grain 14*	12.568	0.881	0.05590	0.00050	494	33	471	17
Grain 16*	12.962	0.682	0.05606	0.00045	479	24	482	18
Grain 18*	13.208	0.696	0.05557	0.00058	470	24	452	23
Grain 19*	13.101	0.688	0.05627	0.00038	474	24	487	15
Grain 20*	12.484	0.660	0.05815	0.00059	497	25	552	25

†Previous age (SHRIMP U-Pb in zircon) reported by Pankhurst et al. (2000).

Concordia Age = 468 ± 2 Ma
 (2 σ , decay-const. errs included)
 MSWD (of concordance) = 0.040,
 Probability (of concordance) = 0.84

Concordia Age = 478 ± 4 Ma†
 MSWD (of concordance) = 0.60

Concordia Age = 464 ± 5 Ma
 (2 σ , decay-const. errs included)
 MSWD (of concordance) = 0.62,
 Probability (of concordance) = 0.43

Table 2.

LA-ICP-MS zircon results for the cordierite-bearing monzogranite of the Sierra de Mazán.

Grain	^{238}U	1σ	^{207}Pb	1σ	$^{206}\text{Pb}/^{238}\text{U}$	1σ	$^{207}\text{Pb}/^{206}\text{Pb}$	1σ
spot	^{206}Pb		^{206}Pb		age		age	
VMA-1018 (P)								
Grain 2*	12.888	0.169	0.05663	0.00044	482	6	481	12
Grain 3	11.960	0.161	0.05841	0.00055	518	7	544	16
Grain 5	10.313	0.136	0.05789	0.00050	597	8	522	14
Grain 6	12.428	0.177	0.05661	0.00044	499	7	483	12
Grain 8	12.191	0.170	0.05747	0.00046	508	7	504	12
Grain 12*	13.265	0.256	0.05707	0.00054	469	9	517	17
Grain 13*	13.283	0.260	0.05614	0.00045	468	9	483	13
Grain 14	13.000	0.260	0.05865	0.00048	478	9	572	14
Grain 16	10.985	0.327	0.05844	0.00063	562	16	551	14
Grain 18*	12.945	0.377	0.05647	0.00060	480	13	482	14
Grain 19	13.689	0.398	0.05664	0.00055	455	13	480	10
Grain 20	11.788	0.352	0.06055	0.00067	525	15	595	11
Grain 21	11.548	0.367	0.05750	0.00058	535	16	510	12
Grain 23	13.573	0.400	0.05616	0.00056	458	13	470	11
Grain 24*	12.846	0.377	0.05687	0.00057	483	14	484	11
Grain 25	10.901	0.325	0.05718	0.00057	566	16	513	12
VMA-1018 (F)								
Grain 2*	13.236	0.133	0.05667	0.00032	470	5	481	12
Grain 3	12.284	0.129	0.05845	0.00045	505	5	544	16
Grain 5	10.592	0.107	0.05793	0.00039	582	6	522	14
Grain 6	12.764	0.147	0.05665	0.00032	486	5	483	12
Grain 8	12.521	0.139	0.05751	0.00034	495	5	504	12
Grain 12	13.169	0.158	0.05701	0.00041	472	5	517	17
Grain 13*	13.186	0.166	0.05608	0.00030	471	6	483	13
Grain 14	12.905	0.170	0.05859	0.00033	481	6	572	14
Grain 16	11.266	0.217	0.05837	0.00036	548	10	551	14
Grain 18*	13.277	0.241	0.05640	0.00033	468	8	482	14
Grain 19	14.039	0.254	0.05657	0.00023	444	8	480	10
Grain 20	12.090	0.236	0.06047	0.00040	512	10	595	11
Grain 21	11.843	0.266	0.05742	0.00027	523	11	510	12
Grain 23	13.920	0.261	0.05609	0.00026	447	8	470	11
Grain 24*	13.175	0.246	0.05680	0.00027	472	8	484	11
Grain 25	11.180	0.216	0.05711	0.00027	552	10	513	12

†Previous age (SHRIMP U-Pb in zircon) reported by Pankhurst et al. (2000).

Concordia Age = 476 ± 6 Ma

(95% confidence, decay-const. errs included)

MSWD (of concordance) = 0.0095,

Probability (of concordance) = 0.92

Concordia Age = 484 ± 3 Ma[†]

MSWD (of concordance) = 0.61

Concordia Age = 470 ± 5 Ma

(95% confidence, decay-const. errs included)

MSWD (of concordance) = 0.26,

Probability (of concordance) = 0.61

Table 2.

LA-ICP-MS zircon results for the biotite-bearing tonalite of the Cerro Toro (Western flank of the Sierra de Famatina)

Grain spot	^{238}U ^{206}Pb	1σ	^{207}Pb ^{206}Pb	1σ	$^{206}\text{Pb}/^{238}\text{U}$ age	1σ	$^{207}\text{Pb}/^{206}\text{Pb}$ age	1σ
FAM-7086								
(P)								
Grain 1	13.304	0.231	0.05486	0.00060	467	8	460	20
Grain 2*	12.557	0.224	0.05716	0.00059	494	8	500	15
Grain 3	12.896	0.212	0.05592	0.00052	481	8	478	11
Grain 4*	12.671	0.247	0.05660	0.00054	490	9	487	12
Grain 7*	12.644	0.200	0.05736	0.00055	491	7	732	63
Grain 8	12.789	0.323	0.05898	0.00082	485	12	1250	171
Grain 9	13.428	0.244	0.05636	0.00066	463	8	538	19
Grain 10*	12.884	0.193	0.05657	0.00052	482	7	476	11
Grain 13	13.486	0.289	0.05697	0.00058	461	10	478	15
Grain 15	12.648	0.271	0.05858	0.00056	491	10	565	13
Grain 18	13.255	0.315	0.05728	0.00062	469	11	522	17
Grain 19*	12.625	0.301	0.05707	0.00054	491	11	563	17
FAM-7086								
(F)								
Grain 1	13.304	0.231	0.05486	0.00060	467	8	460	20
Grain 2*	12.557	0.224	0.05716	0.00059	494	8	500	15
Grain 3	12.896	0.212	0.05592	0.00052	481	8	478	11
Grain 4*	12.671	0.247	0.05660	0.00054	490	9	487	12
Grain 7	12.644	0.200	0.05736	0.00055	491	7	732	63
Grain 8	12.789	0.323	0.05898	0.00082	485	12	1250	171
Grain 9	13.428	0.244	0.05636	0.00066	463	8	538	19
Grain 10	12.884	0.193	0.05657	0.00052	482	7	476	11
Grain 13	13.486	0.289	0.05697	0.00058	461	10	478	15
Grain 15	12.648	0.271	0.05858	0.00056	491	10	565	13
Grain 18	13.255	0.315	0.05728	0.00062	469	11	522	17
Grain 19*	12.625	0.301	0.05707	0.00054	491	11	563	17

*Previous age (SHRIMP U-Pb in zircon) reported by Dahlquist et al. (2008).

Concordia Age = 489 ± 4 Ma

(2σ , decay-const. errs included)

MSWD (of concordance) = 0.0020,

Probability (of concordance) = 0.96

481 ± 4 Ma [95% conf.]†

Wtd. by data-pt errs only, 1 of 8 rej.
MSWD = 0.24

Concordia Age = 489 ± 5 Ma

(2σ , decay-const. errs included)

MSWD (of concordance) = 0.59,

Probability (of concordance) = 0.44

Table 2.

LA-ICP-MS zircon results for the monzogranite NPE-14 of the Achala batholith

Grain spot	^{238}U ^{206}Pb	1σ	^{207}Pb ^{206}Pb	1σ	$^{206}\text{Pb}/^{238}\text{U}$ age	1σ	$^{207}\text{Pb}/^{206}\text{Pb}$ age	1σ
NPE-14 (P)								
Grain 1*	16.373	0.243	0.0540	0.0007	382	5	370	31
Grain 2	16.503	0.271	0.0586	0.0008	379	6	553	31
Grain 3	16.784	0.289	0.0569	0.0007	373	6	486	28
Grain 4*	16.649	0.274	0.0547	0.0007	376	6	399	30
Grain 6*	16.859	0.265	0.0544	0.0008	371	6	389	33
Grain 8	5.030	0.209	0.6004	0.0091	1169	44	4509	22
Grain 9	6.755	0.221	0.4896	0.0075	890	27	4210	22
Grain 11	8.927	0.234	0.4541	0.0068	684	17	4099	22
Grain 13	6.986	0.175	0.4796	0.0072	862	20	4180	22
NPE-14 (F)								
Grain 1*	16.745	0.336	0.0539	0.0006	374	7	367	23
Grain 2	16.878	0.361	0.0586	0.0007	371	8	551	24
Grain 3	17.165	0.378	0.0568	0.0005	365	8	484	19
Grain 4	17.027	0.364	0.0546	0.0005	368	8	396	21
Grain 6*	17.242	0.358	0.0544	0.0006	363	7	386	26
Grain 8	5.144	0.229	0.5997	0.0072	1145	46	4507	17
Grain 9	6.908	0.249	0.4891	0.0059	871	29	4209	18
Grain 11	8.927	0.234	0.4541	0.0068	684	17	4099	22
Grain 13	6.986	0.175	0.4796	0.0072	862	20	4180	22

Concordia Age = 377 ± 3 Ma
 (2 σ , decay-const. errs included)
 MSWD (of concordance) = 0.91,
 Probability (of concordance) = 0.34

Concordia Age = 369 ± 5 Ma
 (2 σ , decay-const. errs included)
 MSWD (of concordance) = 0.48,
 Probability (of concordance) = 0.49

Table 2.

LA-ICP-MS zircon results for the monzogranite DAL-1 of the Achala batholith

Grain spot	^{238}U ^{206}Pb	1σ	^{207}Pb ^{206}Pb	1σ	$^{206}\text{Pb}/^{238}\text{U}$ age	1σ	$^{207}\text{Pb}/^{206}\text{Pb}$ age	1σ
DAL-1 (P)								
Grain 1	18.059	0.436	0.0587	0.0010	347	8	557	36
Grain 3	15.957	0.376	0.0539	0.0008	392	9	367	34
Grain 4	18.776	0.464	0.0596	0.0009	334	8	590	32
Grain 5	15.974	0.388	0.0582	0.0009	391	9	538	33
Grain 6	15.457	0.363	0.0549	0.0008	404	9	408	33
Grain 7	14.948	0.369	0.0541	0.0008	417	10	373	35
Grain 8	16.172	0.402	0.0596	0.0009	387	9	589	33
Grain 9	16.178	0.379	0.0591	0.0009	387	9	570	33
Grain 10	16.712	0.406	0.0547	0.0008	375	9	400	33
Grain 11*	16.248	0.371	0.0548	0.0006	385	9	405	23
Grain 13	15.712	0.348	0.0560	0.0006	398	9	452	22
Grain 14*	16.061	0.346	0.0541	0.0006	389	8	374	23
Grain 18	15.774	0.362	0.0537	0.0005	396	9	358	22
Grain 19*	16.184	0.376	0.0544	0.0006	386	9	389	24
Grain 20	15.345	0.361	0.0553	0.0006	407	9	422	25
DAL-1 (F)								
Grain 1	18.727	0.624	0.0584	0.0006	347	8	557	36
Grain 3	16.547	0.544	0.0536	0.0004	392	9	367	34
Grain 4	19.471	0.657	0.0593	0.0004	334	8	590	32
Grain 5	16.564	0.554	0.0579	0.0005	391	9	538	33
Grain 6	16.028	0.526	0.0546	0.0004	404	9	408	33
Grain 7	15.501	0.523	0.0537	0.0005	417	10	373	35
Grain 8	16.770	0.569	0.0592	0.0005	387	9	589	33
Grain 9	16.776	0.550	0.0587	0.0005	387	9	570	33
Grain 10	17.330	0.579	0.0544	0.0004	375	9	400	33
Grain 11	17.037	0.478	0.0547	0.0004	385	9	405	23
Grain 13	16.475	0.451	0.0559	0.0004	398	9	452	22
Grain 14*	16.841	0.453	0.0540	0.0004	389	8	374	23
Grain 18	16.540	0.465	0.0536	0.0004	396	9	358	22
Grain 19*	16.970	0.481	0.0544	0.0004	386	9	389	24
Grain 20	16.090	0.461	0.0552	0.0005	407	9	422	25

[†]This age is more consistent with that previously reported for granitic rocks of the Achala batholith (e.g., Dorais et al., 1997; Rapela et al., 2008b).

Concordia Age = 387 ± 5 Ma
(2σ , decay-const. errs included)
MSWD (of concordance) = 0.071,
Probability (of concordance) = 0.79

Concordia Age = 372 ± 6 Ma[†]
(2σ , decay-const. errs included)
MSWD (of concordance) = 0.91,
Probability (of concordance) = 0.34

Table 2.

LA-ICP-MS zircon results for the monzogranite ACH-140 of the Achala batholith

Grain spot	^{238}U ^{206}Pb	1σ	^{207}Pb ^{206}Pb	1σ	$^{206}\text{Pb}/^{238}\text{U}$ age	1σ	$^{207}\text{Pb}/^{206}\text{Pb}$ age	1σ
ACH-140 (P)								
Grain 1	16.590	0.161	0.056	0.001	377	4	469	22
Grain 2	17.487	0.180	0.056	0.001	358	4	437	23
Grain 3*	16.797	0.157	0.054	0.001	373	3	392	21
Grain 7*	16.799	0.170	0.054	0.001	373	4	383	24
Grain 8	16.124	0.165	0.055	0.001	388	4	430	21
Grain 10	17.345	0.172	0.057	0.001	361	3	496	22
Grain 11	16.088	0.165	0.055	0.001	389	4	403	22
Grain 13	17.885	0.178	0.074	0.001	351	3	1031	20
Grain 14	16.340	0.177	0.055	0.001	383	4	408	24
Grain 16	16.403	0.156	0.055	0.001	381	4	423	22
Grain 17	17.282	0.170	0.055	0.001	363	3	412	21
Grain 18	16.437	0.167	0.055	0.001	381	4	425	23
Grain 20	16.544	0.190	0.055	0.001	378	4	424	23
ACH-140 (F)								
Grain 1	16.936	0.392	0.0560	0.0007	370	8	454	27
Grain 2	17.851	0.418	0.0552	0.0007	351	8	422	28
Grain 3*	17.148	0.394	0.0541	0.0006	365	8	376	26
Grain 7*	17.149	0.400	0.0539	0.0007	365	8	368	28
Grain 8	16.461	0.385	0.0551	0.0006	380	9	415	26
Grain 10	17.707	0.411	0.0567	0.0007	354	8	480	27
Grain 11	16.552	0.224	0.0544	0.0004	378	5	387	15
Grain 13	18.402	0.243	0.0731	0.0005	341	4	1017	14
Grain 14	16.812	0.235	0.0545	0.0004	372	5	392	17
Grain 16	16.877	0.218	0.0549	0.0003	371	5	407	14
Grain 17	17.781	0.234	0.0546	0.0003	353	5	395	13
Grain 18	16.912	0.227	0.0549	0.0004	370	5	409	16
Grain 20	17.022	0.247	0.0549	0.0004	368	5	407	16

Concordia Age = 373 ± 3 Ma
 (2 σ , decay-const. errs included)
MSWD (of concordance) = 3.3,
Probability (of concordance) = 0.069

Concordia Age = 366 ± 6 Ma
 (2 σ , decay-const. errs included)
MSWD (of concordance) = 0.43,
Probability (of concordance) = 0.51

Table 2.
LA-ICP-MS zircon results for the Los Árboles pluton (Sierra de Fiambalá)

Grain spot	^{238}U ^{206}Pb	1σ	^{207}Pb ^{206}Pb	1σ	$^{206}\text{Pb}/^{238}\text{U}$ age	1σ	$^{207}\text{Pb}/^{206}\text{Pb}$ age	1σ
FIA-17 (P)								
Grain 1a	19.531	0.249	0.05369	0.00062	322	4	358	26
Grain 1b*	19.433	0.266	0.05381	0.00062	323	4	363	26
Grain 3a*	19.320	0.287	0.05352	0.00066	325	5	351	28
Grain 4a	19.923	0.247	0.05361	0.00061	316	4	355	25
Grain 7a*	19.969	0.260	0.05354	0.00067	315	4	352	28
Grain 7b	19.694	0.253	0.05253	0.00068	319	4	309	29
Grain 8a	19.898	0.216	0.05650	0.00069	316	3	472	27
Grain 12a	18.866	0.195	0.05526	0.00065	333	3	423	26
Grain 18a	19.139	0.205	0.05459	0.00061	328	3	395	25
Grain 19a	19.931	0.225	0.05520	0.00062	316	3	421	25
FIA-17 (F)								
Grain 1a*	19.403	0.227	0.05295	0.00035	324	4	326	15
Grain 1b*	19.305	0.245	0.05306	0.00034	326	4	331	14
Grain 3a*	19.193	0.267	0.05278	0.00042	327	4	320	18
Grain 4a*	19.792	0.224	0.05287	0.00033	318	4	323	14
Grain 7a*	19.838	0.238	0.05280	0.00043	317	4	320	18
Grain 7b	19.565	0.231	0.05181	0.00046	321	4	277	20
Grain 8a	19.723	0.218	0.05604	0.00029	319	3	454	12
Grain 12a	18.700	0.198	0.05480	0.00021	336	3	404	9
Grain 18a	18.856	0.111	0.05430	0.00036	333	2	384	15
Grain 19a	19.637	0.135	0.05492	0.00037	320	2	409	15

Concordia Age = 325 ± 10 Ma
(95% confidence, decay-const. errs included)

MSWD (of concordance) = 11.0,
Probability (of concordance) = 0.001

Concordia Age = 322 ± 3 Ma
(95% confidence, decay-const. errs included)

MSWD (of concordance) = 0.45,
Probability (of concordance) = 0.50

Table 2.

LA-ICP-MS zircon results for the Zapata granitic complex (Sierra de Zapata)

Grain	^{238}U	1σ	^{207}Pb	1σ	$^{206}\text{Pb}/^{238}\text{U}$	1σ	$^{207}\text{Pb}/^{206}\text{Pb}$	1σ
spot	^{206}Pb		^{206}Pb		age		age	
ZAP-33 (P)								
Grain 2*	18.697	0.867	0.05319	0.00038	336	15	345	15
Grain 3*	18.738	0.869	0.05273	0.00038	335	15	324	16
Grain 4*	18.403	0.857	0.05335	0.00042	341	15	358	18
Grain 5	17.999	0.838	0.05488	0.00041	349	16	409	17
Grain 6*	18.798	0.871	0.05377	0.00042	334	15	360	17
Grain 7*	18.566	0.872	0.05353	0.00054	338	15	353	24
Grain 9*	18.501	0.857	0.05351	0.00044	339	15	363	18
Grain 12	18.133	0.261	0.05298	0.00051	346	5	341	21
Grain 13	19.207	0.292	0.05517	0.00052	327	5	406	21
Grain 14	18.241	0.263	0.05241	0.00045	344	5	346	19
Grain 15	18.121	0.242	0.05403	0.00035	346	5	381	13
Grain 18	18.596	0.250	0.05285	0.00034	338	4	336	12
Grain 20	18.769	0.271	0.05447	0.00052	335	5	386	21
Grain 23*	18.596	0.280	0.05299	0.00046	338	5	363	22
Grain 25	19.187	0.304	0.05469	0.00060	328	5	413	27
Grain 26*	18.254	0.295	0.05310	0.00068	344	5	374	26
Grain 28	19.094	0.299	0.05355	0.00051	329	5	389	26
Grain 29	18.111	0.289	0.05374	0.00051	346	5	383	25
ZAP-33 (F)								
Grain 2*	19.273	0.655	0.05300	0.00032	326	11	345	15
Grain 3	19.315	0.656	0.05254	0.00032	325	11	324	16
Grain 4*	18.969	0.651	0.05316	0.00037	331	11	358	18
Grain 5	18.552	0.636	0.05468	0.00036	338	11	409	17
Grain 6	19.376	0.659	0.05357	0.00037	324	11	360	17
Grain 7*	19.138	0.667	0.05333	0.00050	328	11	353	24
Grain 9*	19.070	0.647	0.05331	0.00039	329	11	363	18
Grain 12	18.644	0.287	0.05281	0.00049	337	5	341	21
Grain 13	19.748	0.319	0.05500	0.00049	318	5	406	21
Grain 14	18.755	0.289	0.05225	0.00042	335	5	346	19
Grain 15	18.631	0.267	0.05386	0.00031	337	5	381	13
Grain 18*	19.119	0.276	0.05269	0.00029	329	5	336	12
Grain 20	19.298	0.297	0.05430	0.00050	326	5	386	21
Grain 23*	19.144	0.213	0.05292	0.00036	328	4	363	22
Grain 25	19.752	0.240	0.05462	0.00053	318	4	413	27
Grain 26*	18.792	0.238	0.05303	0.00062	334	4	374	26
Grain 28	19.656	0.235	0.05348	0.00043	320	4	389	26
Grain 29*	18.644	0.230	0.05367	0.00043	337	4	383	25

Concordia Age = 340 ± 3 Ma(2 σ , decay-const. errs included)

MSWD (of concordance) = 0.00059,

Probability (of concordance) = 0.98

Concordia Age = 332 ± 3 Ma

(95% confidence, decay-const. errs included)

MSWD (of concordance) = 0.0088,

Probability (of concordance) = 0.93

Table 2.

LA-ICP-MS zircon results for the Huaco granitic complex (Sierra de Velasco)

Grain spot	^{238}U ^{206}Pb	1σ	^{207}Pb ^{206}Pb	1σ	$^{206}\text{Pb}/^{238}\text{U}$ age	1σ	$^{207}\text{Pb}/^{206}\text{Pb}$ age	1σ
HUA-12 (P)								
Grain 3	17.200	0.441	0.05515	0.00065	364	9	419	26
Grain 4	16.956	0.426	0.05779	0.00053	369	9	522	20
Grain 7	16.737	0.451	0.05178	0.00081	374	10	276	35
Grain 8*	16.888	0.440	0.05370	0.00050	371	9	358	21
Grain 9	16.512	0.419	0.05630	0.00062	379	9	464	24
Grain 11*	16.890	0.452	0.05360	0.00045	371	10	354	19
Grain 12	16.772	0.471	0.05691	0.00068	373	10	488	26
Grain 15	18.580	0.521	0.06948	0.00071	338	9	913	21
Grain 18	15.725	0.425	0.07335	0.00081	397	10	1024	22
Grain 19	15.747	0.420	0.05327	0.00048	397	10	340	20
HUA-12 (F)								
Grain 3	18.016	0.253	0.05525	0.00053	348	5	422	21
Grain 4	17.760	0.231	0.05789	0.00037	353	4	526	14
Grain 7	17.531	0.290	0.05187	0.00073	358	6	280	32
Grain 8*	17.688	0.262	0.05379	0.00034	355	5	362	14
Grain 9	17.295	0.233	0.05640	0.00049	362	5	468	19
Grain 11*	17.495	0.186	0.05368	0.00017	358	4	358	7
Grain 12	17.373	0.242	0.05700	0.00051	361	5	491	19
Grain 15	19.246	0.264	0.06958	0.00045	327	4	916	13
Grain 18	16.288	0.185	0.07346	0.00057	384	4	1027	16
Grain 19	16.311	0.170	0.05335	0.00023	384	4	344	10

†This age (LA-ICP-MS U-Pb in monacite) is similar to that reported by [Grosse et al. \(2009\)](#).**Concordia Age = 357 ± 3 Ma[†]**(2 σ , decay-const. errs included)

MSWD (of concordance) = 0.12,

Probability (of concordance) = 0.73

Concordia Age = 368 ± 6 Ma(2 σ , decay-const. errs included)

MSWD (of concordance) = 3.2,

Probability (of concordance) = 0.072

Table 2.
LA-ICP-MS zircon results for the San blas pluton (Sierra de Velasco)

Grain spot	^{238}U ^{206}Pb	1σ	^{207}Pb ^{206}Pb	1σ	$^{206}\text{Pb}/^{238}\text{U}$ age	1σ	$^{207}\text{Pb}/^{206}\text{Pb}$ age	1σ
VEL-6017 (P)								
Grain 1a	18.016	0.217	0.05411	0.00044	348	4	656	46
Grain 4a*	18.622	0.247	0.05371	0.00069	337	4	392	29
Grain 5a*	18.429	0.201	0.05295	0.00043	341	4	345	15
Grain 6a	17.240	0.256	0.05444	0.00055	363	5	443	22
Grain 9a	17.345	0.265	0.05735	0.00085	361	5	575	32
Grain 11a*	18.254	0.240	0.05304	0.00050	344	4	342	18
Grain 13a*	18.701	0.264	0.05335	0.00060	336	5	389	24
Grain 16a	17.912	0.196	0.05278	0.00046	350	4	353	16
Grain 2b	19.486	0.701	0.05742	0.00096	323	11	769	81
Grain 8a	18.453	0.342	0.05280	0.00090	340	6	599	28
Grain 12a*	18.265	0.264	0.05313	0.00063	344	5	1147	42
Grain 17a	18.721	0.285	0.05144	0.00069	335	5	2013	82
Grain 18a	17.911	0.201	0.05829	0.00049	350	4	1378	52
VEL-6017 (F)								
Grain 1a	18.016	0.217	0.05411	0.00044	348	4	656	46
Grain 4a	18.622	0.247	0.05371	0.00069	337	4	392	29
Grain 5a	18.429	0.201	0.05295	0.00043	341	4	345	15
Grain 6a	18.224	0.230	0.05458	0.00047	344	4	443	22
Grain 9a	18.335	0.242	0.05750	0.00079	342	4	575	32
Grain 11a	19.296	0.198	0.05317	0.00040	326	3	342	18
Grain 13a	19.768	0.230	0.05348	0.00053	318	4	389	24
Grain 16a*	18.974	0.233	0.05300	0.00038	331	4	353	16
Grain 2b	19.486	0.701	0.05742	0.00096	323	11	769	81
Grain 8a	19.506	0.335	0.05294	0.00086	322	5	599	28
Grain 12a*	19.307	0.234	0.05326	0.00055	326	4	1147	42
Grain 17a	19.832	0.330	0.05166	0.00064	317	5	2013	82
Grain 18a	18.974	0.239	0.05853	0.00040	331	4	1378	52

[†]Previous age (SHRIMP U-Pb in zircon) reported by Dahlquist et al. (2006).

Concordia Age = 340 ± 2 Ma
(2σ , decay-const. errs included)
MSWD (of concordance) = 0.70,
Probability (of concordance) = 0.40

Mean $^{206}\text{Pb}/^{238}\text{U}$ Age
 340 ± 3 Ma[†]
N= 16/19; MSWD = 1.5
(Error ellipses are 1σ)

Concordia Age = 329 ± 3 Ma
(2σ , decay-const. errs included)
MSWD (of concordance) = 0.33,
Probability (of concordance) = 0.57

Table 2.

LA-ICP-MS zircon results for the Cerro La Gloria (Sierra de Famatina)

Grain	^{238}U	1σ	^{207}Pb	1σ	$^{206}\text{Pb}/^{238}\text{U}$	1σ	$^{207}\text{Pb}/^{206}\text{Pb}$	1σ
spot	^{206}Pb		^{206}Pb		age		age	
FAM-177 (P)								
Grain 2	17.157	0.316	0.05558	0.00058	365	7	444	22
Grain 8*	17.745	0.337	0.05376	0.00059	353	7	359	23
Grain 9	18.072	0.325	0.05541	0.00054	347	6	429	20
Grain 12	17.180	0.284	0.05480	0.00058	365	6	409	14
Grain 15*	17.850	0.290	0.05377	0.00056	351	6	379	13
Grain 18	19.479	0.309	0.06168	0.00061	323	5	676	10
Grain 19	19.242	0.310	0.06003	0.00059	327	5	618	9
FAM-177 (F)								
Grain 2	17.736	0.298	0.05558	0.00036	354	6	444	22
Grain 8*	18.344	0.320	0.05377	0.00039	342	6	359	23
Grain 9	18.682	0.303	0.05542	0.00030	336	5	429	20
Grain 12	17.530	0.501	0.05480	0.00034	358	10	409	14
Grain 15*	18.213	0.517	0.05377	0.00032	345	10	379	13
Grain 18	19.875	0.560	0.06168	0.00030	316	9	676	10
Grain 19	19.633	0.556	0.06003	0.00029	320	9	618	9

†Previous age (SHRIMP U-Pb in zircon) reported by [Alasino et al. \(2012\)](#).**Concordia Age = 353 ± 4 Ma**(2 σ , decay-const. errs included)

MSWD (of concordance) = 0.97,

Probability (of concordance) = 0.32

Cerro La Gloria pluton

(FAM-177)

 349 ± 3 Ma[†]

MSWD = 1.1

Concordia Age = 346 ± 13 Ma

(95% confidence, decay-const. errs included)

MSWD (of concordance) = 9.0,

Probability (of concordance) = 0.003

Table**Table 3a.**

Laser ablation Hf isotope data for igneous dated zircons from Sierras Pampeanas of Argentina (location of samples in Fig. 1 and Table 1).

Sample	Grain	Age (Ma)	$^{176}\text{Hf}/^{177}\text{Hf}$	$\pm (2\sigma)$	$^{176}\text{Lu}/^{177}\text{Hf}$	$\pm (2\sigma)$	$^{176}\text{Yb}/^{177}\text{Hf}$	Age (Ma)	ϵHf (today)	$\pm (2\sigma)$	ϵHf (t)	T _{DM} Hf
<i>Early-Middle Ordovician granitic rocks (Ancasti, Famatina, Valle Fértil, and Mazán mountain ranges)</i>												
ANC-11030a												
4/3[†]												
	ANC11030a_8a	466	0.282464	0.000062	0.001761	0.000100	0.068127	466	-11.4	2.2	-1.5	1.5
	ANC11030a_3a	466	0.282386	0.000041	0.002333	0.000113	0.080279	466	-14.1	1.4	-4.5	1.6
	ANC11030a_2a	466	0.282396	0.000039	0.001887	0.000120	0.075972	466	-13.7	1.4	-4.0	1.7
<i>Average</i>												
FAM-7086												
8/6												
	FAM7086_1b	489	0.282198	0.000043	0.002483	0.000073	0.076713	489	-20.8	1.5	-10.7	2.0
	FAM7086_5a	489	0.282110	0.000035	0.002693	0.000144	0.088002	489	-23.9	1.3	-13.9	2.2
	FAM7086_3a	489	0.281986	0.000030	0.004196	0.000377	0.119129	481	-28.3	1.1	-18.9	2.5
	FAM7086_4a	489	0.282055	0.000065	0.002380	0.000074	0.072752	489	-25.8	2.3	-15.7	2.3
	FAM7086_2b	489	0.282173	0.000037	0.002643	0.000108	0.085036	489	-21.6	1.3	-11.6	2.0
<i>Average</i>												
SVF-577												
13/11												
	SVF577_17a	464	0.282324	0.000061	0.000581	0.000013	0.025969	464	-16.3	2.2	-6.1	1.7
	SVF577_15a	464	0.282375	0.000057	0.000902	0.000040	0.037338	464	-14.5	2.0	-4.5	1.6
	SVF577_13a	464	0.282301	0.000046	0.000466	0.000016	0.020208	464	-17.1	1.6	-6.9	1.8
	SVF577_11a	464	0.282335	0.000036	0.000260	0.000008	0.009712	464	-15.9	1.3	-5.7	1.7
	SVF577_10a	464	0.282366	0.000046	0.000595	0.000037	0.020873	464	-14.8	1.6	-4.7	1.6
	SVF577_8a	464	0.282334	0.000063	0.000434	0.000035	0.016921	464	-16.0	2.2	-5.8	1.7
	SVF577_7a	464	0.282365	0.000067	0.000538	0.000037	0.021245	464	-14.9	2.4	-4.7	1.6
	SVF577_6a	464	0.282380	0.000043	0.000445	0.000022	0.017711	464	-14.3	1.5	-4.1	1.6
	SVF577_1a	464	0.282247	0.000059	0.000375	0.000019	0.011942	464	-19.0	2.1	-8.8	1.9
<i>Average</i>												
VMA-1018												
8/8												
	VEL_1018_9a	476	0.282248	0.000032	0.001231	0.000083	0.056862	476	-19.0	1.1	-8.8	1.9
	VEL_1018_8a	476	0.282324	0.000030	0.002385	0.000276	0.121735	476	-16.3	1.1	-6.4	1.7
	VEL_1018_7a	476	0.282282	0.000034	0.003245	0.000219	0.147306	476	-17.8	1.2	-8.2	1.8
	VEL_1018_6a	476	0.282302	0.000044	0.003756	0.000648	0.145780	476	-17.1	1.6	-7.7	1.8
	VEL_1018_5a	476	0.282283	0.000035	0.001581	0.000157	0.066127	476	-17.8	1.2	-7.7	1.8

VEL_1018_4a	476	0.282349	0.000021	0.001904	0.000171	0.095304	476	-15.4	0.8	-5.4	1.7
VEL_1018_3a	476	0.282253	0.000030	0.002041	0.000031	0.093116	476	-18.8	1.2	-8.9	1.9
VEL_1018_1a	476	0.282356	0.000042	0.001854	0.000089	0.091752	476	-15.2	1.5	-5.2	1.7
<i>Average</i>									-7.3	1.8	

[†] Total number of analyses / number chosen for ϵ Hf calculation.

[§] VEL-6017 defines two Hf compositions populations.

Table 3a (continuation).

Laser ablation Hf isotope data for igneous dated zircons from Sierras Pampeanas of Argentina (location of samples in Fig. 1 and Table 1).

Sample	Grain	Age (Ma)	$^{176}\text{Hf}/^{177}\text{Hf}$	$\pm (2\sigma)$	$^{176}\text{Lu}/^{177}\text{Hf}$	$\pm (2\sigma)$	$^{176}\text{Yb}/^{177}\text{Hf}$	Age (Ma)	ϵHf (today)	$\pm (2\sigma)$	ϵHf (t)	$T_{\text{DM}}\text{ Hf}$
<i>Late-Middle Devonian granitic rocks (Achala batholith)</i>												
DAL-1												
7/7												
	Dal1_8a	372	0.282372	0.000062	0.000822	0.000032	0.038368	372	-14.6	2.2	-6.5	1.8
	Dal1_7a	372	0.282462	0.000032	0.000659	0.000008	0.031781	372	-11.4	1.1	-3.3	1.6
	Dal1_6a	372	0.282427	0.000045	0.000721	0.000045	0.033232	372	-12.7	1.6	-4.7	1.6
	Dal1_4a	372	0.282482	0.000060	0.000756	0.000009	0.037214	372	-10.7	2.1	-2.6	1.4
	Dal1_3a	372	0.282475	0.000033	0.000793	0.000018	0.037658	372	-11.0	1.2	-2.9	1.5
	Dal1_2a	372	0.282498	0.000039	0.000586	0.000021	0.028253	372	-10.1	1.4	-2.0	1.4
	Dal1_1a	372	0.282454	0.000028	0.000591	0.000009	0.027818	372	-11.7	1.0	-3.7	1.5
<i>Average</i>											-3.6	1.5
NPE-14												
7/7												
	NPE_14_3c	369	0.282424	0.000042	0.000790	0.000021	0.041036	369	-12.8	1.5	-4.7	1.6
	NPE_14_3b	369	0.282449	0.000046	0.000779	0.000060	0.039925	369	-11.9	1.6	-3.8	1.5
	NPE_14_3a	369	0.282312	0.000049	0.001181	0.000144	0.048790	369	-16.7	1.7	-8.7	1.8
	NPE_14_2d	369	0.282373	0.000048	0.000691	0.000048	0.035585	369	-14.6	1.7	-6.5	1.7
	NPE_14_2c	369	0.282383	0.000052	0.000682	0.000043	0.034580	369	-14.2	1.9	-6.1	1.7
	NPE_14_2b	369	0.282415	0.000049	0.000708	0.000053	0.036478	369	-13.1	1.7	-5.0	1.6
	NPE_14_2a	369	0.282367	0.000045	0.000895	0.000050	0.037973	369	-14.8	1.6	-6.7	1.7
<i>Average</i>											-5.9	1.6
ACH-140												
10/7												
	ACH140_10a	366	0.282484	0.000023	0.000978	0.000051	0.051003	366	-10.6	0.8	-2.7	1.4
	ACH140_9a	366	0.282468	0.000031	0.001216	0.000036	0.061520	366	-11.2	1.1	-3.4	1.5
	ACH140_8a	366	0.282380	0.000050	0.001339	0.000183	0.055740	366	-14.3	1.8	-6.5	1.7
	ACH140_6a	366	0.282480	0.000030	0.000836	0.000031	0.043617	366	-10.8	1.1	-2.8	1.4
	ACH140_5a	366	0.282454	0.000025	0.000891	0.000017	0.044674	366	-11.7	0.9	-3.8	1.5
	ACH140_2b	366	0.282434	0.000028	0.000893	0.000074	0.048033	366	-12.4	1.0	-4.5	1.5
	ACH140_1a	366	0.282477	0.000025	0.000921	0.000061	0.048627	366	-10.9	0.9	-3.0	1.5
<i>Average</i>											-3.8	1.5
NPE-10												
10/9												
	NPE_10_7a	369	0.282485	0.000033	0.000892	0.000032	0.042838	369	-10.6	1.2	-2.6	1.43

NPE_10_6a	369	0.282371	0.000048	0.000794	0.000048	0.034683	369	-14.6	1.7	-6.6	1.7	
NPE_10_5a	369	0.282423	0.000030	0.001099	0.000069	0.048549	369	-12.8	1.1	-4.9	1.6	
NPE_10_4a	369	0.282447	0.000036	0.000850	0.000020	0.039005	369	-11.9	1.3	-3.9	1.5	
NPE_10_3b	369	0.282493	0.000033	0.000628	0.000051	0.031648	369	-10.3	1.2	-2.3	1.4	
NPE_10_2a	369	0.282464	0.000025	0.001387	0.000056	0.066827	369	-11.3	0.9	-3.5	1.5	
NPE_10_1c	369	0.282453	0.000043	0.001146	0.000016	0.048249	369	-11.7	1.5	-3.8	1.5	
NPE_10_1b	369	0.282500	0.000036	0.000997	0.000013	0.048892	369	-10.1	1.3	-2.1	1.4	
NPE_10_1a	369	0.282475	0.000049	0.000873	0.000033	0.040185	369	-11.0	1.8	-3.0	1.5	
<i>Average</i>											-3.6	1.5

Table 3a (continuation).

Laser ablation Hf isotope data for igneous dated zircons from Sierras Pampeanas of Argentina (location of samples in Fig. 1 and Table 1).

Sample	Grain	Age (Ma)	$^{176}\text{Hf}/^{177}\text{Hf}$	$\pm (2\sigma)$	$^{176}\text{Lu}/^{177}\text{Hf}$	$\pm (2\sigma)$	$^{176}\text{Yb}/^{177}\text{Hf}$	Age (Ma)	ϵHf (today)	$\pm (2\sigma)$	ϵHf (t)	$T_{\text{DM}}\text{Hf}$
<i>Early Carboniferous granitic rocks (Fiambalá, Velasco, Famatina and Zapata mountain ranges).</i>												
FIA-17	8/6											
	FIA17_6b	322	0.282477	0.000074	0.000544	0.000002	0.026722	322	-10.9	2.6	-3.9	1.5
	FIA17_4a	322	0.282493	0.000046	0.001762	0.000147	0.097517	322	-10.3	1.6	-3.5	1.4
	FIA17_3b	322	0.282432	0.000067	0.000916	0.000027	0.045564	322	-12.5	2.4	-5.5	1.6
	FIA17_3a	322	0.282359	0.000068	0.000627	0.000019	0.030277	322	-15.1	2.4	-8.0	1.7
	FIA17_1b	322	0.282469	0.000064	0.000677	0.000011	0.034428	322	-11.2	2.3	-4.2	1.5
	FIA17_1a	322	0.282445	0.000061	0.000557	0.000014	0.027907	322	-12.0	2.16	-5.0	1.6
<i>Average</i>											-5.0	1.6
HUA-12	7/5											
	HUA12_6a	357	0.282523	0.000029	0.001206	0.000169	0.059043	357	-9.3	1.0	-1.6	1.4
	HUA12_5b	357	0.282503	0.000051	0.001274	0.000072	0.065866	357	-10.0	1.8	-2.4	1.4
	HUA12_4a	357	0.282471	0.000040	0.000989	0.000011	0.049964	357	-11.1	1.4	-3.4	1.5
	HUA12_3a	357	0.282405	0.000038	0.001637	0.000033	0.084079	357	-13.4	1.3	-5.9	1.6
	HUA12_1a	357	0.282469	0.000059	0.000771	0.000044	0.041285	357	-11.2	2.1	-3.4	1.5
<i>Average</i>											-3.3	1.5
CHI-17	3/3											
	CHI7_5a	345	0.282363	0.000051	0.001324	0.000140	0.052209	345	-14.9	1.8	-7.6	1.7
	CHI7_4a	345	0.282361	0.000032	0.001481	0.000235	0.062902	345	-15.0	1.1	-7.7	1.7
	CHI7_2a	345	0.282440	0.000028	0.001475	0.000214	0.061438	345	-12.2	1.0	-4.9	1.5
<i>Average</i>											-6.7	1.7
FAM-177	11/9											
	FAM_177_3b	353	0.282605	0.000055	0.001347	0.000027	0.063763	353	-6.4	2.0	1.2	1.2
	FAM_177_6b	353	0.282666	0.000037	0.002280	0.000232	0.098271	353	-4.2	1.3	3.1	1.0
	FAM_177_5b	353	0.282655	0.000040	0.001772	0.000030	0.088599	353	-4.6	1.4	2.8	1.1
	FAM_177_4b	353	0.282607	0.000031	0.001263	0.000027	0.059873	353	-6.3	1.1	1.3	1.2
	FAM_177_4a	353	0.282667	0.000035	0.002556	0.000214	0.121723	353	-4.2	1.2	3.1	1.0
	FAM_177_3a	353	0.282651	0.000038	0.002223	0.000168	0.105691	353	-4.7	1.3	2.6	1.1
	FAM_177_2a	353	0.282632	0.000052	0.001272	0.000140	0.057944	353	-5.4	1.9	2.2	1.1
	FAM_177_1b	353	0.282628	0.000031	0.001679	0.000085	0.079175	353	-5.6	1.1	1.9	1.1

	FAM_177_1a	353	0.282716	0.000034	0.002703	0.000258	0.131327	353	-2.42	1.21	4.8	0.9
<i>Average</i>											2.6	1.1
ZAP-33	12/11											
	ZAP_33_12a	340	0.282409	0.000024	0.000482	0.000017	0.022801	340	-13.3	0.9	-5.9	1.6
	ZAP_33_11a	340	0.282409	0.000031	0.000685	0.000014	0.031634	340	-13.3	1.1	-5.9	1.6
	ZAP_33_10a	340	0.282424	0.000023	0.000577	0.000005	0.026810	340	-12.8	0.8	-5.3	1.6
	ZAP_33_9a	340	0.282379	0.000023	0.000926	0.000024	0.044627	340	-14.4	0.8	-7.0	1.7
	ZAP_33_8a	340	0.282407	0.000044	0.000616	0.000009	0.031501	340	-13.4	1.6	-5.9	1.6
	ZAP_33_7b	340	0.282396	0.000035	0.000576	0.000022	0.027877	340	-13.8	1.2	-6.3	1.7
	ZAP_33_5a	340	0.282438	0.000024	0.000453	0.000002	0.020572	340	-12.3	0.9	-4.8	1.6
	ZAP_33_3b	340	0.282447	0.000032	0.000851	0.000009	0.036220	340	-12.0	1.1	-4.6	1.5
	ZAP_33_3a	340	0.282431	0.000025	0.001165	0.000026	0.048962	340	-12.5	0.9	-5.2	1.6
	ZAP_33_2a	340	0.282394	0.000028	0.000615	0.000017	0.028751	340	-13.8	1.0	-6.4	1.7
	ZAP_33_1a	340	0.282401	0.000040	0.001311	0.000099	0.039749	340	-13.6	1.4	-6.3	1.6
<i>Average</i>											-5.8	1.6
VEL-6017^s	10/10											
	VEL_6017_4a	340	0.282444	0.000057	0.001671	0.000140	0.062118	340	-12.1	2.0	-4.9	1.5
	VEL_6017_1a	340	0.282410	0.000080	0.001217	0.000077	0.050555	340	-13.3	2.8	-6.0	1.6
	<i>Average</i>										-5.4	1.6
	VEL_6017_2a	340	0.282543	0.000057	0.000840	0.000073	0.033059	340	-8.5	2.0	-1.2	1.3
	VEL_6017_1b	340	0.282518	0.000071	0.000879	0.000206	0.040033	340	-9.4	2.5	-2.1	1.4
	VEL_6017_5b	340	0.282619	0.000073	0.000554	0.000007	0.028718	340	-5.9	2.9	1.6	1.2
	VEL_6017_3a	340	0.282574	0.000043	0.000367	0.000006	0.017919	340	-7.5	1.5	0.0	1.3
	VEL_6017_2b	340	0.282591	0.000049	0.000739	0.000033	0.037920	340	-6.9	1.7	0.6	1.2
<i>Average</i>											-0.2	1.3

Table 3b. Laser ablation Hf isotope data for igneous dated zircons from Sierras Pampeanas of Argentina (location of samples in Fig. 1 and Table 1).

Sample	Grain	Age (Ma)	$^{176}\text{Hf}/^{177}\text{Hf}$	$\pm (2\sigma)$	$^{176}\text{Lu}/^{177}\text{Hf}$	$\pm (2\sigma)$	$^{176}\text{Yb}/^{177}\text{Hf}$	Age (Ma)	ϵHf (today)	$\pm (2\sigma)$	ϵHf (t)	$T_{\text{DM}} \text{ Hf}$
<i>Early-Middle Ordovician granitic rocks (Ancasti, Famatina, Valle Fértil, and Mazán mountain ranges)</i>												
ANC-11030a 4/4												
	ANC11030a_4a*	466	0.282190	0.000062	0.002783	0.000135	0.089553	466	-21.1	2.2	-11.5	2.07
	ANC11030a_8a	466	0.282464	0.000062	0.001761	0.000100	0.068127	466	-11.4	2.2	-1.5	1.45
	ANC11030a_3a	466	0.282386	0.000041	0.002333	0.000113	0.080279	466	-14.1	1.4	-4.5	1.59
	ANC11030a_2a	466	0.282396	0.000039	0.001887	0.000120	0.075972	466	-13.7	1.4	-4.0	1.57

ALL TABLES: Hf values histograms below each Table, X = ϵHf (t) and Y = Frequency.

Samples without deleted values are not included in these Tables.

*In blue colour Hf ‘extreme’ values deleted in Table 3a.

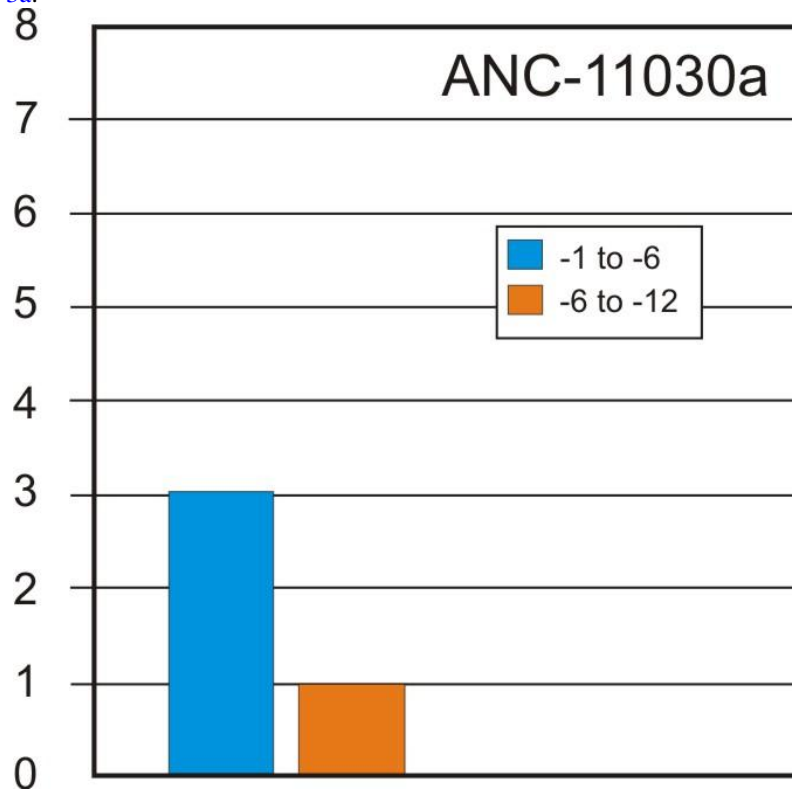


Table 3b (continuation). Laser ablation Hf isotope data for igneous dated zircons from Sierras Pampeanas of Argentina (location of samples in Fig. 1 and Table 1).

Sample	Grain	Age (Ma)	$^{176}\text{Hf}/^{177}\text{Hf}$	$\pm (2\sigma)$	$^{176}\text{Lu}/^{177}\text{Hf}$	$\pm (2\sigma)$	$^{176}\text{Yb}/^{177}\text{Hf}$	Age (Ma)	ϵHf (today)	$\pm (2\sigma)$	$\epsilon\text{Hf} (\text{t})$	$T_{\text{DM}} \text{ Hf}$
FAM-7086	8/8											
	FAM7086_1b	489	0.282198	0.000043	0.002483	0.000073	0.076713	489	-20.8	1.5	-10.7	2.0
	FAM7086_5a	489	0.282110	0.000035	0.002693	0.000144	0.088002	489	-23.9	1.3	-13.9	2.2
	FAM7086_3b	489	0.281864	0.000066	0.004249	0.000176	0.150712	489	-32.6	2.3	-23.1	2.8
	FAM7086_3a	489	0.281986	0.000030	0.004196	0.000377	0.119129	489	-28.3	1.1	-18.9	2.5
	FAM7086_4a	489	0.282055	0.000065	0.002380	0.000074	0.072752	489	-25.8	2.3	-15.7	2.3
	FAM7086_2b	489	0.282173	0.000037	0.002643	0.000108	0.085036	489	-21.6	1.3	-11.6	2.0
	FAM7086_2a	489	0.282367	0.000035	0.001740	0.000072	0.074037	489	-14.8	1.2	-4.5	1.7

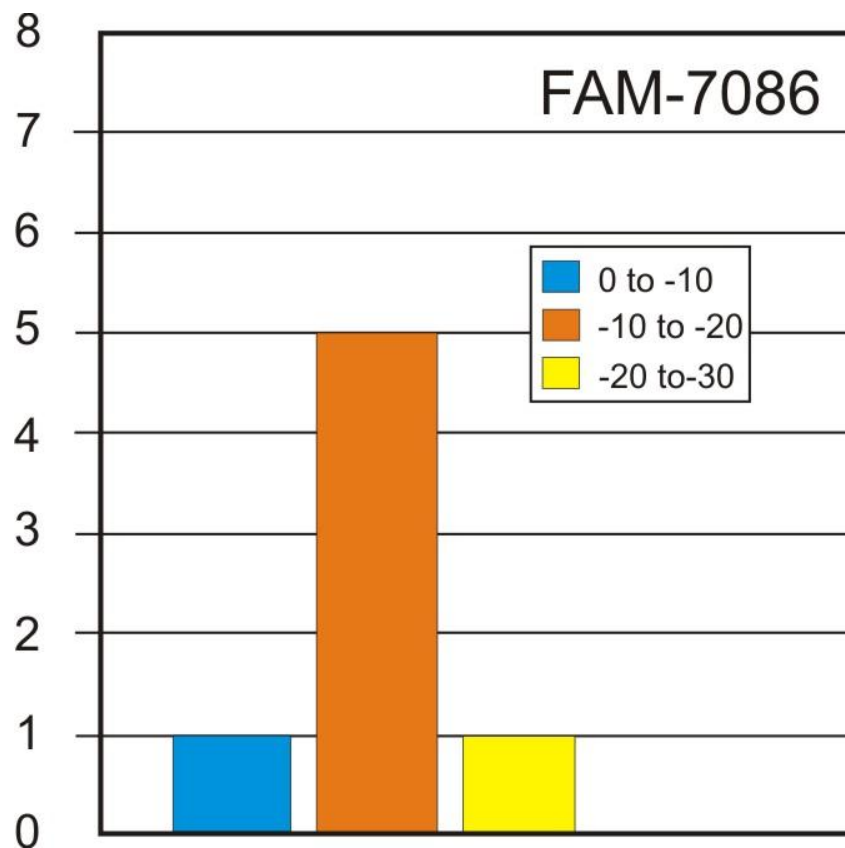


Table 3b (continuation). Laser ablation Hf isotope data for igneous dated zircons from Sierras Pampeanas of Argentina (location of samples in Fig. 1 and Table 1).

Sample	Grain	Age (Ma)	$^{176}\text{Hf}/^{177}\text{Hf}$	$\pm (2\sigma)$	$^{176}\text{Lu}/^{177}\text{Hf}$	$\pm (2\sigma)$	$^{176}\text{Yb}/^{177}\text{Hf}$	Age (Ma)	ϵHf (today)	$\pm (2\sigma)$	$\epsilon\text{Hf} (\text{t})$	$T_{\text{DM}} \text{Hf}$
SVF-577	13/11											
	SVF577_17a	464	0.282324	0.000061	0.000581	0.000013	0.025969	464	-16.3	2.2	-6.1	1.7
	SVF577_15a	464	0.282375	0.000057	0.000902	0.000040	0.037338	464	-14.5	2.0	-4.5	1.6
	SVF577_14a	464	0.282149	0.000047	0.000619	0.000001	0.025898	472	-22.5	1.7	-12.2	2.1
	SVF577_13a	464	0.282301	0.000046	0.000466	0.000016	0.020208	464	-17.1	1.6	-6.9	1.8
	SVF577_11a	464	0.282335	0.000036	0.000260	0.000008	0.009712	464	-15.9	1.3	-5.7	1.7
	SVF577_10a	464	0.282366	0.000046	0.000595	0.000037	0.020873	464	-14.8	1.6	-4.7	1.6
	SVF577_8a	464	0.282334	0.000063	0.000434	0.000035	0.016921	464	-16.0	2.2	-5.8	1.7
	SVF577_7a	464	0.282365	0.000067	0.000538	0.000037	0.021245	464	-14.9	2.4	-4.7	1.6
	SVF577_6a	464	0.282380	0.000043	0.000445	0.000022	0.017711	464	-14.3	1.5	-4.1	1.6
	SVF577_1a	464	0.282247	0.000059	0.000375	0.000019	0.011942	464	-19.0	2.1	-8.8	1.9

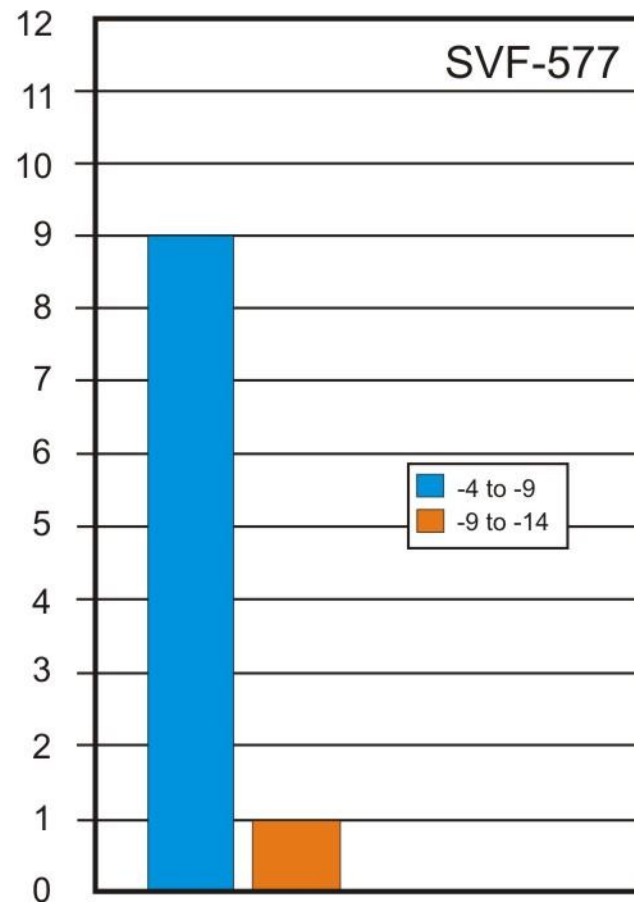


Table 3b (continuation). Laser ablation Hf isotope data for igneous dated zircons from Sierras Pampeanas of Argentina (location of samples in Fig. 1 and Table 1).

Sample	Grain	Age (Ma)	$^{176}\text{Hf}/^{177}\text{Hf}$	$\pm (2\sigma)$	$^{176}\text{Lu}/^{177}\text{Hf}$	$\pm (2\sigma)$	$^{176}\text{Yb}/^{177}\text{Hf}$	Age (Ma)	ϵHf (today)	$\pm (2\sigma)$	ϵHf (t)	$T_{\text{DM}}\text{ Hf}$
<i>Late-Middle Devonian granitic rocks (Achala batholith)</i>												
ACH-140	10/7											
	ACH140_11a	366	0.282264	0.000031	0.001794	0.000083	0.062771	366	-18.4	1.1	-10.7	2.0
	ACH140_10a	366	0.282484	0.000023	0.000978	0.000051	0.051003	366	-10.6	0.8	-2.7	1.4
	ACH140_9a	366	0.282468	0.000031	0.001216	0.000036	0.061520	366	-11.2	1.1	-3.4	1.5
	ACH140_7a	366	0.282086	0.000052	0.003303	0.000076	0.110948	366	-24.7	1.8	-17.4	2.4
	ACH140_8a	366	0.282380	0.000050	0.001339	0.000183	0.055740	366	-14.3	1.8	-6.5	1.7
	ACH140_6a	366	0.282480	0.000030	0.000836	0.000031	0.043617	366	-10.8	1.1	-2.8	1.4
	ACH140_4a	366	0.282128	0.000067	0.002252	0.000065	0.074003	366	-23.2	2.4	-15.6	2.3
	ACH140_5a	366	0.282454	0.000025	0.000891	0.000017	0.044674	366	-11.7	0.9	-3.8	1.5
	ACH140_2b	366	0.282434	0.000028	0.000893	0.000074	0.048033	366	-12.4	1.0	-4.5	1.5
	ACH140_1a	366	0.282477	0.000025	0.000921	0.000061	0.048627	366	-10.9	0.9	-3.0	1.5

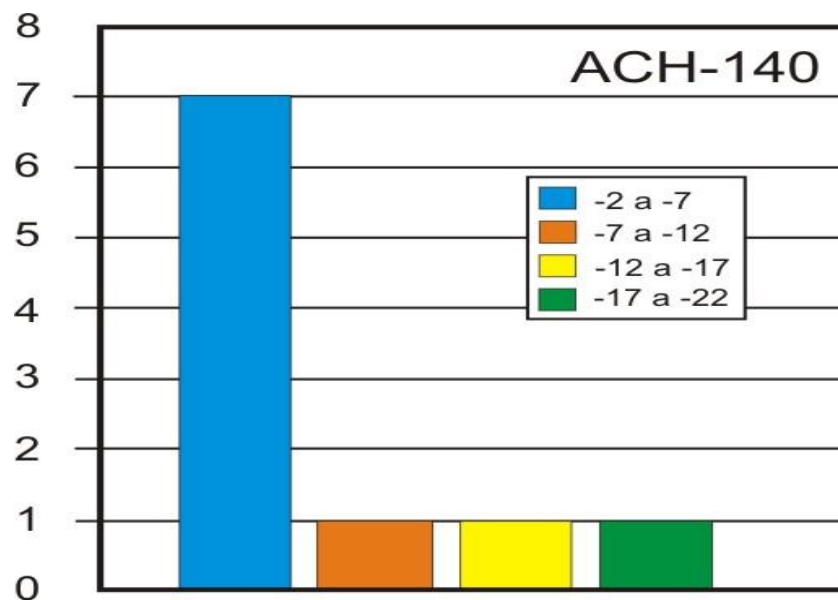


Table 3b (continuation). Laser ablation Hf isotope data for igneous dated zircons from Sierras Pampeanas of Argentina (location of samples in Fig. 1 and Table 1).

Sample	Grain	Age (Ma)	$^{176}\text{Hf}/^{177}\text{Hf}$	\pm (2 s)	$^{176}\text{Lu}/^{177}\text{Hf}$	\pm (2 s)	$^{176}\text{Yb}/^{177}\text{Hf}$	Age (Ma)	ϵHf (today)	\pm (2 s)	ϵHf (t)	$T_{\text{DM}}\text{ Hf}$
<i>Early Carboniferous granitic rocks (Fiambalá, Velasco, Famatina and Zapata mountain ranges).</i>												
FIA-17												
			8/6									
	FIA17_6b	322	0.282477	0.000074	0.000544	0.000002	0.026722	322	-10.9	2.6	-3.9	1.5
	FIA17_4b	322	0.282149	0.000047	0.000619	0.000001	0.025898	322	-22.5	1.7	-15.5	2.2
	FIA17_4a	322	0.282493	0.000046	0.001762	0.000147	0.097517	322	-10.3	1.6	-3.5	1.4
	FIA17_3b	322	0.282432	0.000067	0.000916	0.000027	0.045564	322	-12.5	2.4	-5.5	1.6
	FIA17_3a	322	0.282359	0.000068	0.000627	0.000019	0.030277	322	-15.1	2.4	-8.0	1.7
	FIA17_1b	322	0.282469	0.000064	0.000677	0.000011	0.034428	322	-11.2	2.3	-4.2	1.5
	FIA17_1a	322	0.282445	0.000061	0.000557	0.000014	0.027907	322	-12.0	2.2	-5.0	1.6

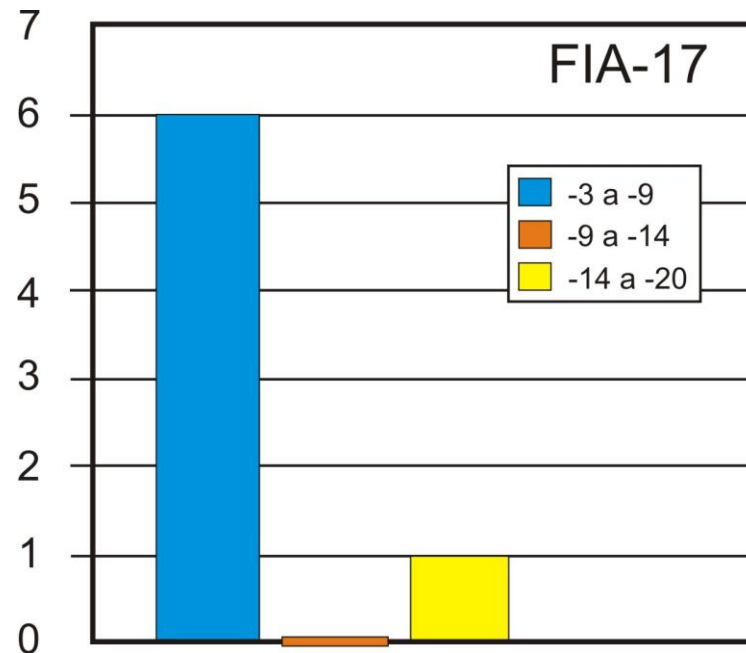


Table 3b (continuation). Laser ablation Hf isotope data for igneous dated zircons from Sierras Pampeanas of Argentina (location of samples in Fig. 1 and Table 1).

Sample	Grain	Age (Ma)	$^{176}\text{Hf}/^{177}\text{Hf}$	\pm (2 s)	$^{176}\text{Lu}/^{177}\text{Hf}$	\pm (2 s)	$^{176}\text{Yb}/^{177}\text{Hf}$	Age (Ma)	ϵHf (today)	\pm (2 s)	ϵHf (t)	$T_{\text{DM}}\text{ Hf}$
HUA-12	7/5											
	HUA12_6a	357	0.282523	0.000029	0.001206	0.000169	0.059043	357	-9.3	1.3	-1.6	1.4
	HUA12_5b	357	0.282503	0.000051	0.001274	0.000072	0.065866	357	-10.0	1.8	-2.4	1.4
	HUA12_5a	357	0.282303	0.000069	0.002333	0.000165	0.080259	357	-17.1	2.4	-9.7	1.9
	HUA12_4a	357	0.282471	0.000040	0.000989	0.000011	0.049964	357	-11.1	1.4	-3.4	1.5
	HUA12_3a	357	0.282405	0.000038	0.001637	0.000033	0.084079	357	-13.4	1.3	-5.9	1.6
	HUA12_2a	357	0.282575	0.000070	0.000736	0.000022	0.038552	357	-7.4	2.5	0.3	1.3
	HUA12_1a	357	0.282469	0.000059	0.000771	0.000044	0.041285	357	-11.2	2.1	-3.4	1.5

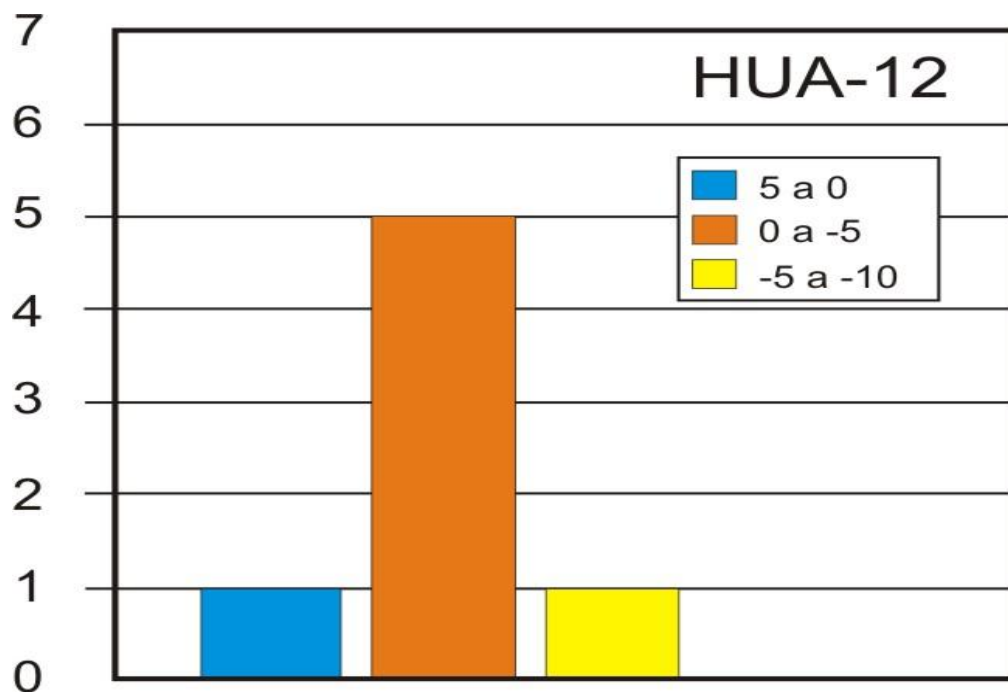


Table 3b (continuation). Laser ablation Hf isotope data for igneous dated zircons from Sierras Pampeanas of Argentina (location of samples in Fig. 1 and Table 1).

Sample	Grain	Age (Ma)	$^{176}\text{Hf}/^{177}\text{Hf}$	$\pm (2\sigma)$	$^{176}\text{Lu}/^{177}\text{Hf}$	$\pm (2\sigma)$	$^{176}\text{Yb}/^{177}\text{Hf}$	Age (Ma)	ϵHf (today)	$\pm (2\sigma)$	ϵHf (t)	$T_{\text{DM}} \text{ Hf}$
FAM-177	11/9											
	FAM_177_3b	353	0.282605	0.000055	0.001347	0.000027	0.063763	353	-6.4	2.0	1.2	1.2
	FAM_177_6b	353	0.282666	0.000037	0.002280	0.000232	0.098271	353	-4.2	1.3	3.1	1.04
	FAM_177_6a	353	0.282493	0.000054	0.003096	0.000118	0.098314	353	-10.3	1.9	-3.2	1.5
	FAM_177_5b	353	0.282655	0.000040	0.001772	0.000030	0.088599	353	-4.6	1.4	2.8	1.1
	FAM_177_5a	353	0.282566	0.000054	0.003304	0.000244	0.127620	353	-7.7	1.9	-0.7	1.3
	FAM_177_4b	353	0.282607	0.000031	0.001263	0.000027	0.059873	353	-6.3	1.1	1.3	1.2
	FAM_177_4a	353	0.282667	0.000035	0.002556	0.000214	0.121723	353	-4.2	1.2	3.1	1.0
	FAM_177_3a	353	0.282651	0.000038	0.002223	0.000168	0.105691	353	-4.7	1.3	2.6	1.1
	FAM_177_2a	353	0.282632	0.000052	0.001272	0.000140	0.057944	353	-5.4	1.9	2.2	1.1
	FAM_177_1b	353	0.282628	0.000031	0.001679	0.000085	0.079175	353	-5.6	1.1	1.9	1.1
	FAM_177_1a	353	0.282716	0.000034	0.002703	0.000258	0.131327	353	-2.4	1.2	4.8	0.9

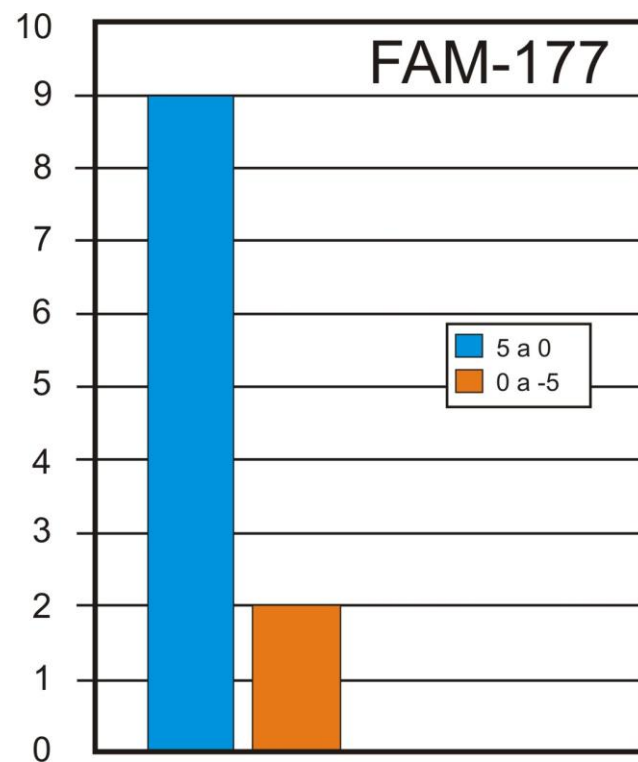


Table 3b (continuation). Laser ablation Hf isotope data for igneous dated zircons from Sierras Pampeanas of Argentina (location of samples in Fig. 1 and Table 1).

Sample	Grain	Age (Ma)	$^{176}\text{Hf}/^{177}\text{Hf}$	$\pm (2\sigma)$	$^{176}\text{Lu}/^{177}\text{Hf}$	$\pm (2\sigma)$	$^{176}\text{Yb}/^{177}\text{Hf}$	Age (Ma)	ϵHf (today)	$\pm (2\sigma)$	ϵHf (t)	$T_{\text{DM}} \text{ Hf}$
ZAP-33	12/11											
	ZAP_33_12a	340	0.282409	0.000024	0.000482	0.000017	0.022801	340	-13.3	0.9	-5.9	1.6
	ZAP_33_11a	340	0.282409	0.000031	0.000685	0.000014	0.031634	340	-13.3	1.1	-5.9	1.6
	ZAP_33_10a	340	0.282424	0.000023	0.000577	0.000005	0.026810	340	-12.8	0.8	-5.3	1.6
	ZAP_33_9a	340	0.282379	0.000023	0.000926	0.000024	0.044627	340	-14.4	0.8	-7.0	1.7
	ZAP_33_8a	340	0.282407	0.000044	0.000616	0.000009	0.031501	340	-13.4	1.6	-5.9	1.6
	ZAP_33_7b	340	0.282396	0.000035	0.000576	0.000022	0.027877	340	-13.8	1.2	-6.3	1.7
	ZAP_33_6a	340	0.282196	0.000034	0.000602	0.000007	0.027530	377	-20.8	1.2	-13.4	2.1
	ZAP_33_5a	340	0.282438	0.000024	0.000453	0.000002	0.020572	340	-12.3	0.9	-4.8	1.6
	ZAP_33_3b	340	0.282447	0.000032	0.000851	0.000009	0.036220	340	-12.0	1.1	-4.6	1.5
	ZAP_33_3a	340	0.282431	0.000025	0.001165	0.000026	0.048962	340	-12.5	0.9	-5.2	1.6
	ZAP_33_2a	340	0.282394	0.000028	0.000615	0.000017	0.028751	340	-13.8	1.0	-6.4	1.7
	ZAP_33_1a	340	0.282401	0.000040	0.001311	0.000099	0.039749	340	-13.6	1.4	-6.3	1.6

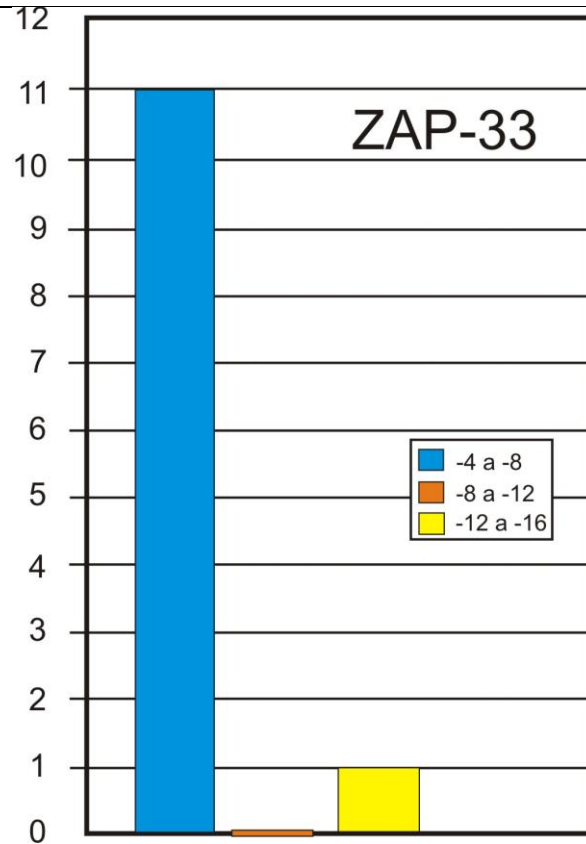


Table 4.
Whole-rock Nd isotopes for Early-Middle Ordovician metaluminous plutonic rocks

Sample	Litology	Ages	Sm (ppm)	Nd (ppm)	$^{147}\text{Sm}/^{144}\text{Nd}$	$(^{143}\text{Nd}/^{144}\text{Nd})_{\text{today}}$	$(^{143}\text{Nd}/^{144}\text{Nd})_t$	$\epsilon\text{Nd}(t)$	T_{DM}^{\dagger} (Ga)
VCA-7037	Granodiorite	473	1.60	6.20	0.1592	0.512226	0.511733	-5.8	1.7
VCA-7038	Granodiorite	473	3.70	20.2	0.1098	0.512113	0.511773	-5.0	1.6
VCA-7040	Granodiorite	473	4.20	22.3	0.1144	0.512112	0.511758	-5.3	1.6
VCA-7039	Granodiorite	473	4.90	22.3	0.1323	0.512191	0.511781	-4.8	1.6
FAM-7086	Tonalite	473	14.2	59.4	0.1445	0.512172	0.511724	-5.9	1.7
FAM-7083	Monzogranite	473	7.70	36.6	0.1264	0.512270	0.511878	-2.9	1.4
RLC-243	Granodiorite	473	5.50	28.3	0.1172	0.512122	0.511759	-5.3	1.6
GUA-253	Tonalite	473	5.00	20.9	0.1455	0.512214	0.511763	-5.2	1.6
GUA-252	Aplite	473	1.80	5.40	0.1983	0.512370	0.511756	-5.3	1.6
MIS-259	Tonalite	473	8.80	40.0	0.1336	0.512200	0.511786	-4.7	1.6
PUL-244	Granodiorite	473	7.30	36.5	0.1213	0.512183	0.511807	-4.3	1.5
ELE-206	Monzogranite	473	6.10	26.0	0.1424	0.512173	0.511732	-5.8	1.7
NAC-257	Monzogranite	473	3.80	18.4	0.1264	0.512159	0.511767	-5.1	1.6
OLT-279	Monzogranite	473	4.90	19.1	0.1560	0.512221	0.511738	-5.7	1.6
OLT-282	Monzogranite	473	5.20	24.2	0.1292	0.512142	0.511742	-5.6	1.6
PAS-272	Granodiorite	473	5.50	27.5	0.1198	0.512119	0.511748	-5.5	1.6
SVF-577	Hbl-rich Gabbro	473	10.1	38.7	0.1582	0.512242	0.511752	-5.4	1.6
ANC-11022	Monzogranite	473	3.90	16.8	0.1412	0.512212	0.511779	-3.3	1.5
ANC-11030a	Tonalite	473	6.00	30.2	0.1198	0.512233	0.511863	-5.0	1.6
<i>Average</i>		473				0.511770	-5.1	1.7	

Age average (473 Ma) was obtained from range of values (484-463 Ma) reported by Dahlquist et al. (2008). Average Nd isotopic composition excludes a few extreme values below -7.0 obtained from S-type granites. $(^{143}\text{Nd}/^{144}\text{Nd})_t$ CHUR = 0.512029, with $t = 473$ Ma.

NOTES: 1. Early-Middle Ordovician data from Pankhurst et al. (1998, 2000) and Dahlquist et al. (2008, 2010). ANC-11030a from Dahlquist et al. (2012), Early Carboniferous data from Dahlquist et al. (2010), and Middle-Late Devonian data from this work, excepting ACH-5, ACH-15, ACH-23, ACH-25 (Rapela et al., 2008b). 2. The decay constants used in the calculations are the values $\lambda^{147}\text{Sm} = 6.54 \times 10^{-12} \text{ year}^{-1}$ recommended by the IUGS Subcommision for Geochronology (Steiger and Jaeger, 1977). Epsilon-Nd (ϵNd) values calculated using the following CHUR parameters (Goldstein et al., 1984; Jacobsen and Wasserburg, 1980): $(^{143}\text{Nd}/^{144}\text{Nd})_{\text{today}} = 0.512638$; $(^{143}\text{Sm}/^{144}\text{Nd})_{\text{today}} = 0.1967$. t = time used for the calculation of the isotopic initial ratios.

[†] T_{DM} = calculated according to De Paolo et al. (1991).

[§]VCA-6017 = SPB-9.

[#]CHI-7 produce an irreal T_{DM} value of -1.4 Ga.

Table 4 (continuation).

Whole-rock Nd isotopes for Late-Middle Devonian granitic rocks

Sample	Litology	Age	Sm (ppm)	Nd (ppm)	$^{147}\text{Sm}/^{144}\text{Nd}$	$(^{143}\text{Nd}/^{144}\text{Nd})_{\text{today}}$	$(^{143}\text{Nd}/^{144}\text{Nd})t$	$\epsilon\text{Nd(t)}$	T_{DM}^{\dagger} (Ga)
DAL-1	Felsic Granodiorite	369	11.5	57.7	0.1203	0.512200	0.511910	-5.0	1.5
ACH-140	Monzogranite	369	5.50	26.8	0.1248	0.512216	0.511915	-4.9	1.5
NPE-6	Monzogranite	369	8.80	43.3	0.1223	0.512152	0.511858	-6.0	1.6
NPE-14	Monzogranite	369	10.2	55.5	0.1112	0.512112	0.511843	-6.3	1.6
NPE-10	Bt-Ap bodies	369	159	709.	0.1358	0.512202	0.511875	-5.7	1.6
NPE-5	Bt-rich granite	369	17.6	87.6	0.1214	0.512148	0.511855	-6.0	1.6
ACH-154	Felsic Granodiorite	369	13.6	97.9	0.0841	0.512033	0.511830	-6.5	1.6
ACH-155	Monzogranite	369	8.90	50.2	0.1066	0.512104	0.511849	-6.2	1.6
ACH-5	Monzogranite	369	3.70	19.7	0.1128	0.512233	0.511961	-4.0	1.4
ACH-25	Monzogranite	369	6.20	32.5	0.1159	0.512239	0.511960	-4.0	1.4
ACH-23	Tonalite	369	6.40	39.0	0.1000	0.512341	0.512100	-1.2	1.2
ACH-15	Tonalite	369	7.10	35.9	0.1191	0.512354	0.512067	-1.9	1.3
<i>Average</i>		369					0.511919	-4.8	1.5

Age average (369 Ma) was obtained from ages reported in [Table 1](#). Average excluding the tonalites, ACH-23 and 15 (see discussion in the text). ACH-155, NPE-5, 6, 10, and 14 from [Dahlquist et al. \(submitted JSAES\)](#).

Table 4 (continuation).

Whole-rock Nd isotopes for Early Carboniferous granitic rocks

Sample	Lithology	Age	Sm (ppm)	Nd (ppm)	$^{147}\text{Sm}/^{144}\text{Nd}$	$(^{143}\text{Nd}/^{144}\text{Nd})_{\text{today}}$	$(^{143}\text{Nd}/^{144}\text{Nd})_{\text{t}}$	$\epsilon\text{Nd(t)}$	T_{DM}^{\dagger} (Ga)
FIA-3	Monzogranite	341	12.1	67.1	0.1090	0.512351	0.512108	-1.8	1.3
FIA-8	Monzogranite	341	11.9	64.0	0.1124	0.512320	0.512069	-2.5	1.3
FIA-17	Monzogranite	341	12.1	51.5	0.1420	0.512434	0.512117	-1.6	1.2
FIA-18	Monzogranite	341	12.5	52.0	0.1453	0.512458	0.512134	-1.3	1.2
FIA-22	Monzogranite	341	11.2	61.7	0.1097	0.512406	0.512161	-0.7	1.2
HUA-4	Monzogranite	341	4.60	20.1	0.1383	0.512338	0.512029	-3.3	1.4
HUA-6	Monzogranite	341	10.2	46.5	0.1326	0.512365	0.512069	-2.5	1.3
HUA-7	Monzogranite	341	9.80	43.6	0.1359	0.512335	0.512032	-3.3	1.4
HUA-12	Monzogranite	341	10.5	49.1	0.1293	0.512352	0.512063	-2.6	1.3
HUA-13	Monzogranite	341	9.20	44.8	0.1241	0.512318	0.512041	-3.1	1.4
SBP-6	Monzogranite	341	17.0	82.1	0.1252	0.512234	0.511955	-4.8	1.5
SBP-9 [†]	Monzogranite	341	9.60	47.5	0.1222	0.512395	0.512122	-1.5	1.2
SBP-10	Monzogranite	341	16.8	73.9	0.1374	0.512537	0.512230	0.6	1.1
SBP-15	Monzogranite	341	11.1	59.5	0.1128	0.512365	0.512113	-1.7	1.2
ZAP-26	Monzogranite	341	17.1	92.3	0.1120	0.512258	0.512008	-3.7	1.4
ZAP-27	Monzogranite	341	18.6	69.6	0.1616	0.512430	0.512069	-2.5	1.3
ZAP-29	Monzogranite	341	15.1	64.5	0.1415	0.512366	0.512050	-2.9	1.3
ZAP-33	Monzogranite	341	9.70	46.3	0.1266	0.512306	0.512023	-3.4	1.4
CHI-7	Monzogranite	341	6.62	14.8	0.2700	0.512663	0.512060	-2.7	1.3
FAM-177	Monzogranite	341	9.47	53.5	0.1070	0.512403	0.512164	-0.7	1.2
<i>Average</i>		341				0.512081	-2.3	1.3	

Age average (341 Ma) was obtained from ages reported in [Table 1](#).

Table 5.

Major and trace element data for the plutonic rocks with Hf and Nd isotopes data (location of samples in Fig. 1 and Table 1).

Samples	Early-Middle Ordovician Plutonic Rocks			Middle-Late Devonian Plutonic Rocks				Early Carboniferous Plutonic Rocks					
	SVF-577	FAM-7086	ANC-11030a	ACH-140	DAL-1 Felsic Gda	NPE-10	NPE-14	FIA-17	HUA-12	CHI-17	FAM-177	SBP-09	ZAP-33
Lithology	Gb	Tn	Tn	Mzg	Bt-Ap-rich bodies	Mzg	Mzg	Mzg	Mzg	Mzg	Mzg	Mzg	Mzg
<i>wt. %</i>													
SiO ₂	42.58	62.73	60.92	73.07	69.16	32.83	70.98	74.50	73.30	74.20	75.05	71.83	71.86
TiO ₂	1.28	0.64	0.80	0.22	0.49	2.77	0.36	0.07	0.19	0.03	0.21	0.38	0.25
Al ₂ O ₃	19.05	17.16	18.25	14.11	15.14	14.29	14.78	11.98	13.39	12.84	12.66	13.57	13.10
Fe ₂ O ₃ ^t	5.19	6.48	5.51	2.08	0.00	0.00	0.00	1.45	2.27	1.05	2.13	3.09	2.41
FeO ^t	9.01	N.D. [†]	N.D. [†]	N.D.	3.24	17.02	2.00	N.D.	N.D.	N.D.	N.D.	N.D.	N.D.
MnO	0.23	0.15	0.13	0.04	0.13	0.41	0.04	0.02	0.05	0.04	0.03	0.05	0.04
MgO	6.87	2.22	1.42	0.39	0.74	5.03	0.50	0.03	0.15	0.05	0.18	0.33	0.19
CaO	12.25	3.23	4.86	0.93	1.08	6.67	0.71	0.64	0.84	0.49	0.83	1.15	1.06
Na ₂ O	1.69	3.61	3.95	2.71	3.62	0.20	3.07	3.29	3.18	3.71	3.59	3.29	3.06
K ₂ O	0.52	2.76	1.84	5.32	4.33	7.05	5.40	4.92	5.19	5.08	5.03	5.39	5.70
P ₂ O ₅	0.21	0.05	0.26	0.28	0.43	5.39	0.30	0.02	0.14	0.02	0.04	0.21	0.07
LOI (%)	0.98	1.03	0.7	0.60	0.88	1.04	1.09	1.66	1.63	1.66	0.19	0.70	1.73
Total	99.86	100.06	98.64	99.76	99.24	92.71*	99.23	98.58	100.33	99.16	99.94	99.99	99.47
<i>ppm</i>													
Cs	0.2	10.1	21.3	12.3	33.2	102.5	9.5	10.1	31.7	16.2	1.5	31.1	11.5
Rb	3.3	176	78	330	551	1500.2	345.9	650	450	716	107	470	372
Sr	205	122	405	68	65.8	12.7	82.3	9	60	9	65	63	74
Ba	70	152	282	175	154.7	148.3	334.1	31	251	16	448	155	74
La	15.6	73.9	21.8	24.5	59.1	829.8	54.6	53.2	51.6	7.78	84.1	52.1	53.4
Ce	54	171	44.7	55.3	133.2	1899.9	133.2	121	120	23.1	175	117	118
Pr	nd	15.8	5.71	7.05	16.2	236.7	16.4	13.7	13.4	3.06	17.1	13.6	13.2
Nd	38	59.4	20.8	24	59.5	888.2	61.8	51.5	49.1	17.5	53.5	47.5	46.3
Sm	9.38	14.2	4.5	5.07	12.3	195.3	11.9	12.1	10.5	6.23	9.47	9.58	9.71
Eu	1.58	1.75	2.05	0.503	0.8	8.8	1	0.186	1.19	0.131	0.94	0.898	1.01
Gd	nd	15.3	4.37	4.02	9	148.8	7	12.4	8.05	7.32	7.39	8.21	8.65

Tb	1.7	3.14	0.67	0.7	1.4	23.6	0.9	2.86	1.62	1.91	1.15	1.39	1.79
Dy	N.D.	21.9	3.97	3.88	7.5	126.7	4.3	19.1	9.59	13.1	5.71	8.04	10.6
Ho	N.D.	4.9	0.82	0.67	1.3	21.8	0.7	3.93	1.74	2.59	1.06	1.46	1.99
Er	N.D.	15.6	2.45	1.82	3.2	53.9	1.6	12.7	5.19	8.33	3.16	4.22	5.85
Tm	N.D.	2.73	0.38	0.26	0.5	7.6	0.2	2.05	0.819	1.55	0.46	0.655	0.909
Yb	5.54	16.5	2.58	1.6	2.9	44.7	1.3	13.1	5.23	10.6	2.77	4.2	5.72
Lu	0.79	2.6	0.42	0.211	0.4	6.3	0.2	1.83	0.741	1.6	0.39	0.59	0.838
U	0.1	4.37	1.09	5.42	12.6	187	3.7	20.7	6.2	56.5	1.9	6.04	7.17
Th	0.4	37	5.18	18.5	47.2	673.6	47.8	77.1	30.1	20.2	17	46.1	28.4
Y	58	145	21.6	19.5	35.6	616.6	18.1	130	54.2	105	26.9	45.8	57.9
Nb	5	29	11.8	20.2	60.6	276.1	22.8	68.3	33.1	30.4	15.6	37.3	34.9
Zr	120	210	838	146	239.6	2580.8	203.5	168	191	69	191	261	248
Hf	3.6	5.3	18.4	4.3	7.4	79.6	6	7.4	5.6	5.1	5.8	7.5	6.9
Ta	0.2	2.28	0.86	1.57	8.6	21.3	1.8	7.86	4.93	13.9	0.78	6.08	4.3
Ga	21	23	22	23	32	54	23	26	24	30	19	23	21
<i>M</i>	3.32	2.91	1.64	1.22	1.27	4.06	1.22	1.46	1.32	1.37	1.44	1.45	1.45
<i>T_{Zr}(°C)</i>		933		792	833	833	822	792	807	817	799	827	821

NOTES: 1. Early-Middle Ordovician geochemistry data from [Pankhurst et al. \(2000\)](#) and [Dahlquist et al. \(2008\)](#), Early Carboniferous geochemistry data from [Dahlquist et al. \(2010\)](#), and Middle-Late Devonian geochemistry data from [Dahlquist et al. \(submitted JSAES\)](#). 2. ACH-140 sample analyzed at ACTLABS. NPE-10, NPE-14 and DAL-1 analyzed at Washington State University. 3. $T_{Zr} = 12,900 / [2.95 + 0.85 M + \ln(496,000 / Zr^{melt})]$, where D^{Zr} , zircon/melt = $(496,000 / Zr^{melt})$, is the ratio of Zr concentrations (ppm) in zircon to that in the saturated melt; *M* is a compositional factor that accounts for dependence of zircon solubility on SiO₂ and peraluminosity of the melt [(Na+K+2·Ca)/Al · Si], all in cation fraction]. The geothermometer is calibrated for *M* = 0.9 to 1.7. Equation and Zr concentrations (ppm) in zircon (= 496,000 ppm) from [Miller et al. \(2003\)](#).

*Low total is attributed to the high F content.

†N.D. = not determined.

Gb = Gabbro, Tn = Tonalite, Gd = Granodiorite, Monzogranite = Mzg.